



University of
Stavanger

Faculty of Science and Technology

MASTER'S THESIS

Study program/ Specialization: Petroleum Engineering/ Reservoir Technology	Spring semester, 2014 Open / Restricted access
Writer: Hans Marius Roscher (Writer's signature)
Faculty supervisor: Leif Larsen	
Thesis title: Reservoir characterization through numerical models	
Credits (ECTS): 30	
Key words: Reservoir characterization Lavrans field Numerical model Pressure Transient Analysis Re-interpretation	Pages: 54 + enclosure: 0 Stavanger, June 13 th / 2014 Date / year

Abstract

Numerical models have been generated for two DST's run in the Ile and Tilje formations in the exploration wells 6406/2-2 and 6406/2-4SR in the Lavrans field located in the mid-Norwegian sea at Haltenbanken. DST 2 in well 6406/2-2 was run in March 1996, and DST 1 in well 6406/2-4SR in January 1999. Several models, with basis in geological maps, are made for each test and compared to geological data to confirm consistency. As part of the re-interpretation a series of numerical models were run for each test to recognize and understand formation properties near and around the wellbore.

The well 6406/2-4SR in the Tilje formation is found to be located in a complex formation with several permeable and impermeable faults and/or compartments surrounding the well. Two possible models are found to give a good match. One composite model with compartments of different permeability built outside the previous compartment. The second model is a flow channel going in circles around the well varying in width of the channel, also with several permeable and impermeable faults present in channel.

According to pressure trends all models show that well 6406/2-2 in the Ile formation is located in a truncated channel which is also consistent with geological map. The channel is easily located in the map but it is not as wide as the map indicates, only 160 ft wide, and 50 ft -80 ft north from the well an impermeable fault is present, sealing the channel in that end while it's open in the south going direction. After 1050 ft the channel opens up towards the west.

Numerical models give a good indication of possible flow patterns or formation layouts in the reservoir due to the flexibility of the model. It allows modifying reservoir model condition to understand different behavior of pressure response. A composite model for 6406/2-2 DST 2 was run to show the flexibility of the numerical models and also underline how important it is to be critical when choosing models.

Lavrans has many isolated segments (compartments) due to tight faults and fractures combined with shale zones that isolate the sand layers. The same trend is observed through pressure transient analysis and numerical models run in Ecrin Kappa Sapphire. Pressure transient tests and numerical models for all cases are generated in Ecrin Sapphire.

Acknowledgement

While working on this thesis I have received as much help as I needed from my faculty supervisor, Leif Larsen. I would like to thank my supervisor for great assistance with this project, first helping me find an appropriate subject and later with guidance, advice and also giving me confidence in my work.

I would also like to thank Yakov Shumakov. Despite being very busy in his position as Reservoir Domain Champion (in Schlumberger) he took time to help and guide me when I needed assistance.

Table of Contents

Abstract	ii
Acknowledgement	iii
Table of Contents	iv
1 Introduction	1
1.1 Background	1
1.2 Objectives	2
1.3 Scope of work	2
2 Lavrans field	3
2.1 Brief information and geological structure	5
2.2 Overview of performed well test operations	6
3 Well test analysis	7
3.1 Data quality assurance and quality control	8
3.2 Flow regimes	9
3.2.1 Early time period	9
3.2.2 Middle time period	9
3.3.3 Late time period	10
3.3 Basic theory of well test interpretation	11
3.4 Pressure Transient Analysis	13
3.4.1 Wellbore storage	14
3.4.2 Flow capacity	17
3.4.3 Radius of investigation	17
3.5 Numerical models	18
3.5.1 Top structure maps of Lavrans field	18
4 Re-interpretation of performed well test on Lavrans	19
Well 6406/2-2	20
Well 6406/2-4SR	36
5 Conclusion and recommendation	46
5.1 Conclusion	46
5.2 Recommendation	47

References.....48

1 Introduction

1.1 Background

Reservoir characterization is a process of describing variations in rock and fluid properties related to the reservoir. Well testing may provide important information related to reservoir pressure, reservoir size, distance from well to boundaries, type of boundaries (permeable/impermeable), heterogeneities in reservoir, flow rates, formation condition, productivity index. Well tests are good for geological modeling through analyzing pressure transient tests to identify reservoir characteristics and boundaries. Reservoir parameters found from pressure transient analysis (PTA) is then used to update geological models and to see if it is consistent with already known data.

Pressure behavior of constant rate drawdown in a well is the main source used to identify a reservoir model. This is done by drilling a well and testing it following a well test procedure. Pressure transient test are designed to create pressure disturbance in reservoir by controlled flow periods known as drawdown and buildup tests. These two periods are a result of production from reservoir as rate changes, constant rate (well shut) for buildup and variable rates (producing reservoir effluent) for drawdowns. Presence of wellbore storage, skin effects, production history (if any) and rate changes will distort important features in pressure and rate responses.

In Lavrans field a re-interpretation of performed well test are conducted. Numerical models are used to identify new possible flow patterns and test leakage through faults (if present). Using existing pressure/rate data from historical production and a geological map to outline faults and fractures a numerical model is created.

1.2 Objectives

Objectives of master thesis are:

- Evaluate pressure transient analyses in Lavrans field using numerical approach together with geological information.
- Understand numerical modeling and how it may be used on previous well test data to enhance interpretation of data.
- Increase knowledge on formation present in Lavrans field using new interpretation techniques on known field data. Identify possible compartments and boundaries around two of the wells tested in Lavrans field.

1.3 Scope of work

Formation in Tilje and Ile are tested through two exploration wells in Lavrans field and selected to investigate possible geological models present. Re-interpretation of performed well tests is conducted using Ecrin Kappa Sapphire software.

Several numerical models are generated and evaluated, and the most consistent models are presented with description of the models and geology.

2 Lavrans field

Information about field and formations are collected from Norwegian Petroleum Department's pages and from *Dolberg 2011*. Lavrans field is located in Haltenbanken west and about 5-10 km south east of Kristin on 850 – 950 ft water depth. In Lavrans there are three wells drilled with two or more DST's run each well. Field is well studied by Statoil (earlier Saga Petroleum) and was proven back in 1994-95. All wireline logs indicate good hydrocarbon zones in all three wells, but after executing pressure test analysis the conclusion have been that Lavrans consists of many smaller compartments with a fracture network connecting them to some extent. Communications between the compartments are not shown to be satisfying enough to bring Lavrans to production. One option have been to do a production test by sending the well effluent from Lavrans to a nearby production facility (Kristin), but the cost/investment versus risk have been found too high.

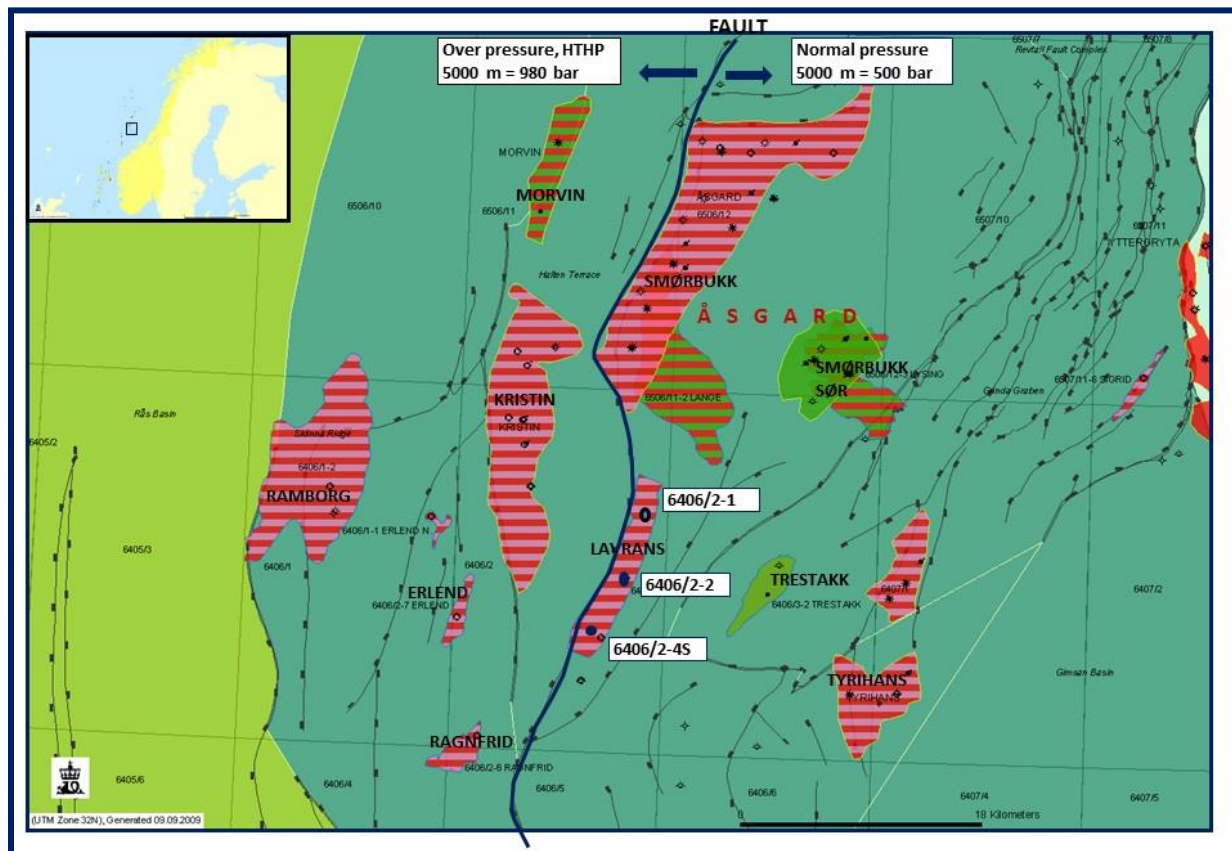


Figure 1: Location of wells in Lavrans including surrounding fields

Lavrans has many isolated segments (compartments) due to tight faults and fractures combined with shale zones that isolate the sand layers. Between 14500 ft and 16500 ft the fault and fractures are normally tight due to quartz diagenesis in fault/fracture zones.

2.1 Brief information and geological structure

Lavrans field consists of the following six formations:

- Garn: Consists of medium to coarse grained sandstone, moderately to well sorted sandstones. Mica rich zones are present and sandstone is occasionally carbonate-cemented. Depositional environment from delta front with active fluvial and wave influence processes recognized. Thickness of 130 – 350 ft.
- Ile: Consists of fine to medium (and occasionally coarse) grained sandstones with thin laminated siltstones and shales. The grains go from fine in the bottom to more coarse further up. Mica rich zones are present and carbonate-cemented stringers occur. Depositional environment from tidal deltas or coastline settings. Thickness of 213 – 236 ft.
- Not: Consists of claystones upwards into fine grained sandstones. Mica rich zones are present and sandstone is occasionally carbonate-cemented, both locally. Depositional environment from lagoons or sheltered bays in the lower part and costal front sediments further up. Thickness of 49 – 121 ft.
- Tofte: Consists of poorly sorted coarse grained sandstone with high quartz content (90%) in the thicker parts of formation. Depositional environment from fan deltas where sandstone were deposited eastwards with an uplift to the west. Thickness from 131 – 213 ft.
- Tilje: Consists of very fine to coarse grained sandstone interbedded with shales and siltstones. High clay content in bottom sandstones with shale. Depositional environment are nearshore with a gradual transition to continental environments eastwards. Thickness of around 328 – 492 ft.
- Åre: Consists of alternating sandstones (fine to coarse grained) and claystones, claystones are interbedded with coals and coaly claystones. Depositional environment are coastal plain to delta deposits with swamps and channels. Thickness of 984 – 1640 ft.

Åre being the oldest formation in the field and coal in this formation is the source rock. Hydrocarbons in Lavrans are trapped in several compartments, where sandstones are dominating and the compartments are separated by shale layers.

2.2 Overview of performed well test operations

Available for this thesis there have been several Drill Stem Tests (DST) run in each of the three separate wells. Two wells have been used for the numerical models. From petrophysical logs there are known to be bad borehole quality in well 6406/1-1R (Lehne 2013), so the other two wells are chosen for re-interpretation. There are two DST run in 6406/2-2 (DST 1 and DST 2) and also two DST's run in 6406/2-4SR (DST 1 and DST 2). Thickness and porosity are assumed to be constant through the tested zones. Composite models, where permeability changes from section to section, are described further down and also equations used to keep porosity constant. A numerical model is combined with geological maps and used for reconstruction of major faults and fractures. All maps referred to is in a position so that North is located up, South is down, east is left and west is right.

When using a numerical model it is very important that the interpreter is critical when choosing models, and when geological data is available it must not be ignored or overlooked. So when a formation with clear faults and open channels are present we cannot design a cylindrical composite model and expect it to be a good reflection of the reservoir. The goal of pressure transient analysis (PTA) is to find flowpaths and locate faults/fractures

Flow rate is not representing entire changes in bottom hole flowing pressure so a perfect match in history plot will not be achievable. The gas rate were probably measured by orifice plate and simplified in PanSystem, which was the software used in the original analyses. Different techniques may be used to increase the resolution of gas flow rate, but it is not done for these numerical analyses.

3 Well test analysis

Well testing is getting less used from time to time due to new technology and methods popping up, but it only tend to last for some years until once again they understand the value of well testing. The two major concerns regarding well tests for exploration and appraisal wells are environmental issues and the high cost. The importance of well test analysis in reservoir characterization will keep increasing together with the understanding of geology, new interpretation techniques and development of improved downhole gauges and flowmeters. However for wider testing and identification of bigger fracture networks a well test (drill stem test) is needed.

Well test analysis is the process of recovering reservoir information from pressure data using well test. There is no unique solution in the analysis so to narrow down the amount of solutions well test analysis may be combined with more information from e.g. logging or geology. Well tests are used for identifying skin, effective permeability and investigating the geology and connectivity of boundary systems as it expands away from the well bore. During a well test a pressure disturbance generated in reservoir is recorded by a gauge either downhole, bottom hole pressure (BHP), or at surface, well head pressure (WHP). Pressure disturbance is an effect of producing (drawdown) and shutting in (buildup) reservoir at surface using surface well test equipment. A standard well test consists of a clean-up, initial build up, main flow and a final buildup, which can be described like this:

- Clean up – first draw down with purpose to make the well clean of any drilling or completion fluids present in wellbore and clean the perforations.
- Draw down (DD) – open well at constant rate giving a decrease in BHP.
- Build up (BU) – shut in well giving an increase in BHP.

Data obtained will give information about both the well and reservoir tested:

- Well description (for tested interval): production index (PI) and skin
- Reservoir description; average/effective permeability, heterogeneities (fractures, layering, properties), boundaries shape and distance, average and initial pressure

For finding skin, effective permeability and boundaries in larger reservoirs there are still no good replacement for well-testing. Effects of skin zone and damaged zone are important to address before starting analyzing data.

After shutting in the well at surface liquid will continue to flow in to the wellbore since wellbore pressure is lower than reservoir pressure, called afterflow. Afterflow stops when pressure downhole is equalized, same pressure in reservoir and wellbore. DST will reduce the effect of afterflow by shutting in the well downhole.

For well tests the depth of investigation (radius of investigation) increases with the duration/length of the test. To identify boundaries far away from well the reservoir need to be tested for a longer time period while observing the pressure response.

There are three main things making the difference between good and bad outcome from well test analysis. For better analysis the following may be improved; recording of data (better signals), interpretation techniques and models to better represent geology (more complex)

3.1 Data quality assurance and quality control

Quality Assurance (QA) and Quality Control (QC) are important to execute for verifying the reliability of recorded data. This should be the starting point of any pressure transient analysis (PTA) and data acquired at all stages of exploration, appraisal, (development) and fluid production should be subjected to QC/QA procedures. Quality of data depends on the design and production process involved in collecting the data.

Derivative overlay may be used to see development in wellbore or reservoir over a different time periods, so it is a way of monitoring well performance. By comparing two or more derivatives (from BU's) it is easier to identify radial flow regime and spot dynamic changes. It is also a good method to control the consistency of rate measurement between data sets.

Evaluating wellbore quality after completion to make sure skin damage and semi perforated formations is not mixed up which will affect the reservoir model. In some cases only a few or none perforations may reach through to formation due to a presence of thicker cement layers (than calculated for) between casing/liner and formation. The effects seen on pressure data will look similar to skin damage and it's hard to separate identify which one that is present without knowing history of the well.

Position (downhole or surface) of rate- and pressure measurement equipment will affect data recordings. It is hard to get good rate measurements whether rate measurement equipment are mounted on surface or downhole, but pressure recorded downhole are reliable. Pressure recorded with constant rate (BU) is the best data to use for interpretation and modelling. With downhole shut-in and good pressure data the different flow regimes should be clear enough to identify (if present).

Deconvolution lets the interpreter access a greater radius of investigation so it is a good tool to use when looking at DST's, but the biggest improvement will be when used on longer tests (permanent downhole pressure gauges).

The superposition principle is important for well test analysis and reservoir engineering in general. Superposition in space is used to show/represent different boundaries in reservoirs while superposition in time is used to determine rate response from reservoir. Since Lavrans is a gas reservoir (gas flow) the superposition principle is not applicable in general, superposition is limited to linear systems only, but at high pressures there is no problem. (Horne 2002)

3.2 Flow regimes

Theory, in the following chapters, is based on information from Schlumberger 2002 and 2006, Larsen 2011 and various SPE papers. In this section the most common observed flow regimes relevant for Lavrans field will be described. One or more of them may be observed in the same well. A PTT is normally divided into three periods, 1-early time period, 2-middle time period and 3-late time period. Each time period is dominated and/or affected by different flow regimes

1. Wellbore storage, skin and transition period before infinite acting radial flow (IARF)
2. IARF, Flow periods before IARF are due to wellbore storage and skin, while flow rates in sandface (physical interference between formation and wellbore) increase slowly before reaching constant rate.
3. Boundary conditions (fractures)

3.2.1 Early time period

Wellbore storage

The afterflow of fluids into wellbore after well is shut in at wellhead. This is the wellbore storage (WBS) effect. Identifying and recognizing this effect in data is important, and also knowing when it can be neglected. It is possible to reduce WBS effect in deep vertical well by using downhole tester valve. To reduce the WBS effect as much as possible (from hours to minutes) it is important to install the downhole gauge close to perforations. Higher up in well, closer to surface, means there will be more liquid re-injection which again will effect gauge recordings. The first analysis of WBS dominated BU's was introduced by Gladfelter et al. (Gladfelter 1955), and after that a variety of methods using different techniques have been proposed. WBS shows up as a unit slope at the start of the PTT.

Skin

The skin effect describes the condition of a well, whether it is damaged or stimulated. It is normally seen on pressure response and described as an additional pressure drop near the well.

3.2.2 Middle time period

It is important to identify the Infinite Acting Radial Flow (IARF) during the test, when flow in reservoir is radial and not influenced by outer boundaries. The term *Infinite Acting* describes the reservoir looking infinite in size since i.e. no outer boundary effects are seen. Sometime during a well test the flow will be radial and not influenced by any outer boundaries, which is one of the bases for interpreting the test. Reaching radial flow during a well test will simplify the mathematical solution of diffusivity equation so interpretation becomes less complicated. This is also the flow regime used to identify flow capacity (permeability-thickness) which is one of the main objectives with a well test.

3.3.3 Late time period

Boundaries and flow restrictions in formation

In most formations the fractures have a dominant direction, but the density of fractures varies throughout the formation. Fractures intersecting wellbore with dip angles less than 90° , radial flow will be observed before other flow regimes, followed by a combination of radial and formation linear flow regimes. With declining pressure in a fracture system the matrix contribution becomes more significant. Microfractures and small cavities in the rock may increase the scales of permeability. Partially penetrating fractures crossing parts of formation and fully penetrating fractures behaves different on a PTT and their effects must be identified. (Kuchuk 2013)

If the situation in *Figure 2* occurs in Lavrans' formations it may be one situation disturbing the effective permeability. Permeability from test $k_{test} = \sqrt{k_y * k_x}$ may show much lower values than core data due to core data being local and only showing a fraction of what is actually tested.

If drainage area is unsymmetrical then more of the reservoir is seen in one of the directions. In the situation from *Figure 2* the reservoir will be more drained in y-direction than x-direction, so an elliptical area of investigation may be present. Linear flow may occur if large-scale horizontal anisotropy is present parallel to k_y (y-direction).

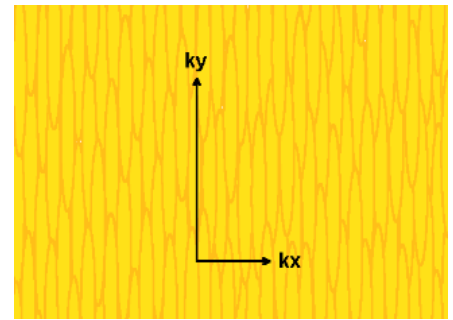


Figure 2: Horizontal anisotropy from depositional architecture

3.3 Basic theory of well test interpretation

Drawdown and buildup tests

The theory behind interpretation of homogeneous isotropic reservoirs is based on line source solution to the radial diffusivity equation developed by Theis (Theis 1935). This solution assumes the source (a well) has an infinitesimally small geometrical line (radius) and it is flowing at constant rate.

Pressure (oilfield units) at time t and distance (from well) r :

$$p(r, t) = p_i - 141.2 \frac{Q\mu}{kh} \left[-0.5Ei\left(\frac{-\varphi\mu C_t r^2}{kt}\right) \right]$$

Where the exponential integral is:

$$Ei(-x) = - \int_{-x}^{\infty} \frac{e^{-u}}{u} du$$

For the line-source solution, the dimensionless pressure, p_D , the dimensionless time, t_D , and the dimensionless radius, r_D is defined:

$$p_D = (p_i - p) \frac{kh}{141.2Q\mu}$$

$$t_D = 0.0002637 \frac{kt}{\varphi\mu C_t r_w^2}$$

$$r_D = \frac{r}{r_w}$$

If the Ei-function solution is rearranged, it can be rewritten using *dimensionless* variables.

$$p_{D(r_D, t_D)} = -Ei\left(-\frac{r_D^2}{4t_D}\right)$$

Approximating by a ln-function for $t_D > 100$ and $r = r_w$ (where p is observed)

$$p_{D(t_D)} = \frac{1}{2} \ln(t_D + 0.80907)$$

Showing the most basic form when IARF is reached. Pressure is proportional to ln of time and will be used for interpreting drawdown tests.

Using the line source solution in log-log coordinates together with type curve matching the interpretation of drawdown tests can be done. Type curve matching can be done manually, on a computer or algorithmically in semi-log coordinates.

Since drawdown tests have a drawback due to production and variable rates (and pressure), the main focus is on buildup tests where rates are constant. During a buildup (BU) test the well is shut in and flow rates are zero. If any previous production/testing are done on reservoir, this must be considered and included when buildup test is interpreted (superposition). A BU is based on recorded pressure data at constant rate (well shut-in) as a function of time after well is shut in. BU tests are the best way to determine near well boundaries, skin and flow capacity (properties) due to the constant rate. During a BU the pressure will increase in a similar way as it decreased during the drawdown (DD), but due to changing skin and dynamic effect it will not be equal.

With derivatives in addition to pressure plot it is much easier to identify the different flowregimes.

3.4 Pressure Transient Analysis

Pressure transient analysis (PTA) involves the analysis of pressure changes generated in the reservoir over a certain time period. The collected data is applied to a mathematical model together with basic reservoir data (tested interval, reservoir height and fluid details). In Lavrans it has been conducted three singlewell test where the measured pressure responses are used to determine the average (effective) properties in drained area of the tested formation. Near-wellbore region in a well will always dominate drawdown and buildup pressure transient behavior. The depth of a near-wellbore region depends on well location, whether the well intersects fractures or not.

Interpretation methodology of a test is quite standard but will not provide one unique solution. There are several factors affecting the outcome of PTA. For better analysis the following may be improved; recording of data (better signals), interpretation techniques and models to better represent geology (more complex) Several of the sources of uncertainty are presented by Horne. Even though the uncertainties reduce the confidence of answers obtained, it is still one of the few effective methods for direct reservoir characterization. (Horne 1995)

Shape of derivative at early, middle and late time in a flow period behave so differently that they are very helpful for interpretation which is not always the case for pressure change. Since the derivative is calculated and not measured there are several factors that may affect the shape of the curve and rate history will have the biggest impact. Some effects may be easier to identify than others; frequency of data recordings, gauge accuracy, time/pressure errors during different flow periods. End effects are one of the affecting things that may be hard to identify together with pressure trend in reservoir

3.4.1 Wellbore storage

Gringarten type curves (Gringarten 1979) are a good and powerful method for PTA. Through the type curves plotted, a solution of diffusivity equation with given conditions are presented. Type curves are then used for comparing well test data in the same plot. In the Gringarten type curve, the time is plotted as t_D/C_D , and the dimensionless wellbore storage coefficient and the skin factor are combined into a parameter $C_D e^{2s}$. Each value of the parameter $C_D e^{2s}$ in *Figure 3* describes a pressure response having a different shape.

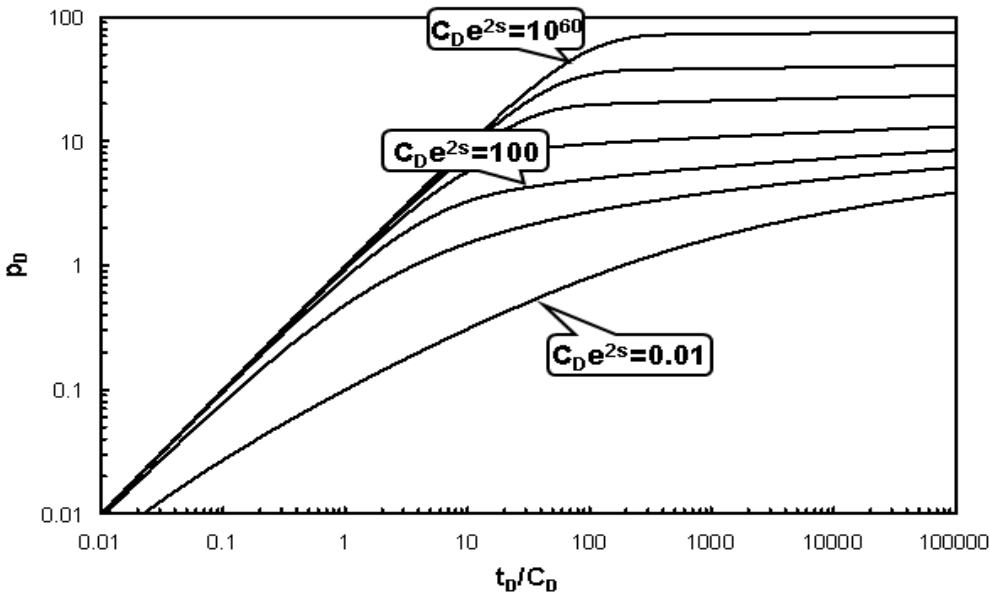


Figure 3: Pressure type curves.

The longer a wellbore storage lasts, the longer unit slope extends before breaking over to radial flow. The effect last until the pressure between wellbore and formation are equalized. Skin is also one important factor affecting the unit slope (same time period as WBS).

Today well tests are interpreted using a log-log plot where pressure is plotted as a function of time. On a log-log plot it is possible to recognize WBS effects, skin/transition zone, radial flow period and boundary effects. When adding pressure derivative to the log-log plot the visual interpretation of the plot becomes easier. Pressure derivative is defined as $p' = \frac{d(\Delta p)}{d(\ln \Delta t)}$ where Δp is the pressure change and Δt is the elapsed time.

Change in WBS is more normal in wells with high GOR due to mass exchange between liquid phase and gas phase. When a well is shut in and shut-in pressure rises liquids may be forced back into formation to an equilibrium height. This will affect the pressure differential between a gauge and the formation.

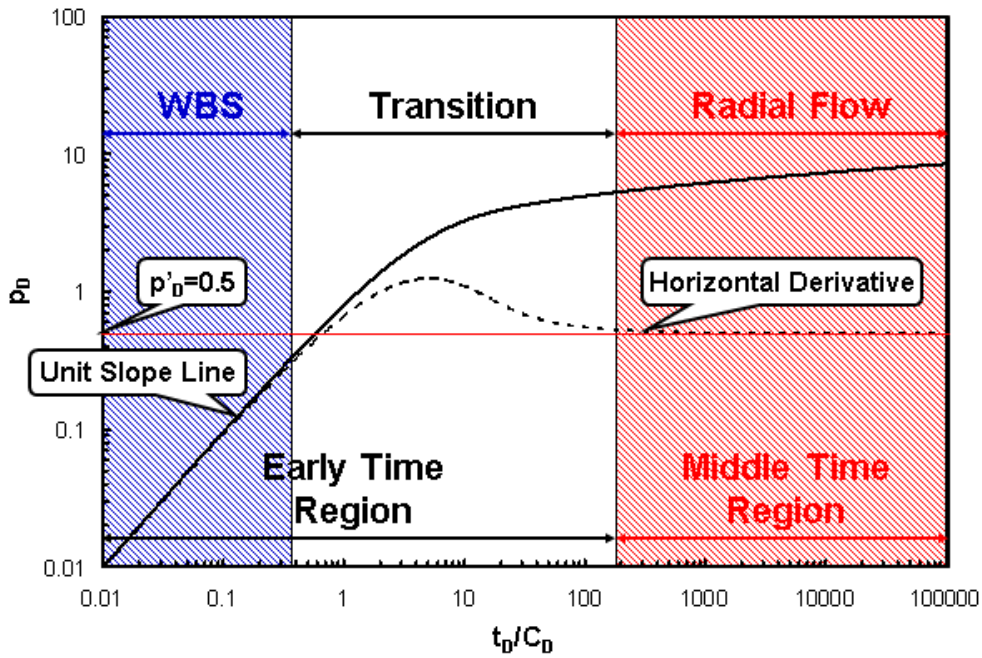


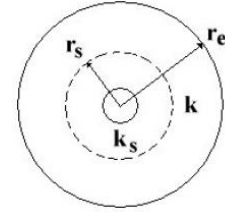
Figure 4: Different events occurring during a well test.

Figure 4 shows a log-log plot of pressure and derivate vs time. In this plot it is easy to recognize WBS by the unit slope line for both curves. The curving just after the first (transition zone) straight line shows skin effect. The horizontal line in middle time region is where radial flow occurs. Late radial flow may show total reservoir heterogeneity. After aligning horizontal and unit slope part of field data and type derivative a value of $C_D e^{2s}$ that best matches data is selected.

Skin

The skin effect describes the condition of a well, whether it is damaged or stimulated. It is often shown and described as an additional pressure drop near the well. Skin factor is described by Hawkins (Hawkins 1956) equation:

$$S = \left(\frac{k}{k_s} - 1 \right) \ln \frac{r_s}{r_w}$$



Where k_s and r_s are permeability and radius of damaged formation respectively.

A positive skin value indicates damaged well or falloffs/solid-deposition near wellbore which will “slow down” pressure increase/decrease recorded. A negative skin value indicates higher permeability near wellbore and intersecting fractures can be one of the reasons for this. Again negative skin is an increased pressure drop during DD, also the reservoir responses are quicker seen/recorded in wellbore.

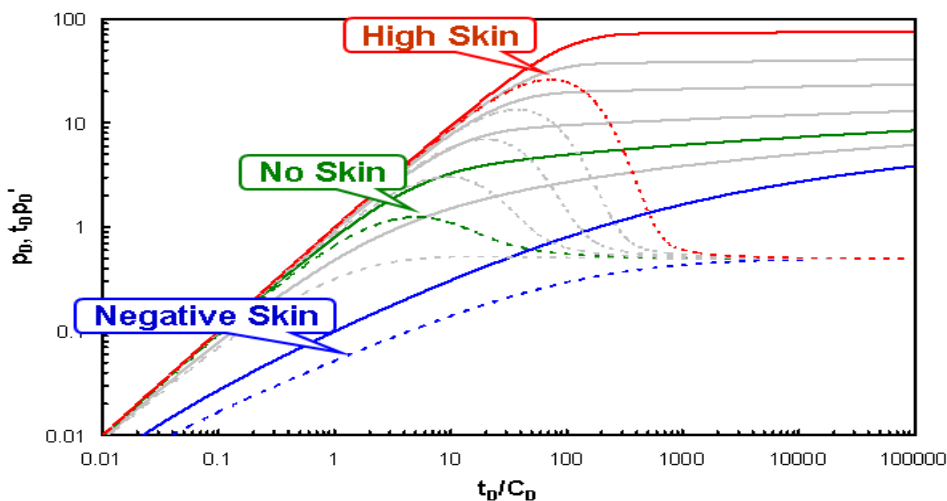


Figure 5: Estimation of skin factor

Skin factor may be estimated qualitatively by the shape of the pressure and pressure derivative response.

High skin factor: The pressure derivative rises to a maximum and then falls sharply before flattening out for the Middle Time Region (MTR). The pressure curve rises along a unit slope then flattens out quickly.

Little or no skin factor: The pressure derivative rises to a maximum, and then falls only slightly before flattening out for the MTR.

Negative skin factor: The pressure derivative approaches a horizontal line from below. The pressure and pressure derivative both leave the unit slope line early, but take a long time to reach the MTR

3.4.2 Flow capacity

Permeability–thickness

Permeability is the most important parameter to test/retrieve during a well test and it controls reservoir (and well) performance. It can be absolute or effective, vertical or horizontal. For a producing reservoir the effective permeability is the main interest. Permeability describes the formations ability to transmit fluids and it is defined as a formation property independent of the fluid. There are several different methods to measure permeability, but the main sources for average effective permeability are well tests and production tests. Other methods that may be used are permeability from logs, cores, core and logs (combined) and wireline formation testing. Permeability from logs/cores need to be calculated and are normally used to compare against permeability from PTT.

Permeability-thickness (kh) is a key factor in the flow potential for a well, and therefore the main goal with a well test is to obtain the best possible value for kh . It's used for a large number of reservoir calculations like future well performance, recovery potential (secondary and tertiary) and different well stimulation processes. One way to find kh is to calculate is from semi-log plot of *time vs. pressure* :

$$kh = \frac{C * q * B * \mu}{m}$$

Where C is a constant (162.6 for oilfield units), B is formation factor and m is the slope from a semi-log plot.

3.4.3 Radius of investigation

The radius of investigation gives an indication of how far into the formation a pressure transient signal has traveled from the well as a two-way event, for instance to a sealing fault and back. The distance depends on rock and fluid properties present in the formation. For PTA the radius of investigation can be used to estimate the distance from the wellbore to specific effects present in the formation. There are several definitions of *Radius of investigation* but since it is beyond the scope of this thesis it will not be discussed any further.

3.5 Numerical models

In numerical models a numerical solution of a well test is used for analysis and interpretation. This is done by using a numerical simulator, in this case Ecrin Kappa Sapphire, which simulates exact pressure response for the tested well. Ecrin Kappa defines numerical models as this: “*Numerical models are used for geometries beyond the scope of analytical models. This is predominantly 2D but with 3D refinement where needed. The most complex numerical model to date solves the problem of fractured horizontal wells*”. For this thesis 2D refinement has been used with the bases in geological top structure map of Lavrans field.

Output from the simulator is used for numerical well test analyses. The advantage with numerical analysis for this case is the possibility to use new models which are consistent with geological data. All cases analyzed include an analytical reservoir model and one or more numerical flow models. Fine characterization of reservoir and geological information are used to determine heterogeneity of reservoir and to build a base model for the numerical well test. It is difficult to choose correct model for detection of boundaries due to the occurrence of them. Boundaries will only be reflected in pressure data after a certain time (duration) of testing. The base model is not fixed/final and will be adjusted throughout the analysis if needed.

One of the crucial points in reservoir modelling is that several different models may equally match the same pressure data. For the analysis to be satisfying a correct model to fit pressure data must be selected. One other important point with analytical and numerical approaches are the interpreters, which models that are best suited for pressure data may be influenced by personal opinions and experience.

There are no standard reservoirs, some may be similar but never 100% match. So that means for every reservoir a specific mathematical model is needed. A mathematical model will never give a perfect match to the analytical model with recorded pressures due to the infinite accuracy of model. Errors may be reduced, but never eliminated, by accurate pressure measurement devices. Choosing the correct model does not mean that all errors are eliminated, when using a simple mathematical model for a complex reservoir behavior errors may still be present, stated by Watson in 1988. A model with too many parameters fixed to it will result in larger errors within the parameters. One option to minimize error is to use a hierarchical approach to model selection which is demonstrated by Watson. The method provides a systematic and quantitative procedure for analysis and model selection. It demonstrates how consistent reservoir data and measured data are. (Watson 1988)

3.5.1 Top structure maps of Lavrans field

Resolution on numerical models are higher than resolution in geological maps so for the more detailed models, especially in 6406/2-4SR, the geological data is not much help. The area around well confirms a complex fault structure, so for models generated this structure is assumed to be present also in a smaller scale. The scale used on geological map is a rough estimate. It is a reliable source with some uncertainties to it.

4 Re-interpretation of performed well test on Lavrans

Both well tests are interpreted using a conventional analytical and a numerical approach. The analytical approach is meant as an example to show the restrictions there are to analytical models. In *Figure 6* is the geological map used for analysis, it is zoomed out to present location of both wells and formation around them. In the sections further down the map is zoomed in to better present the actual models.

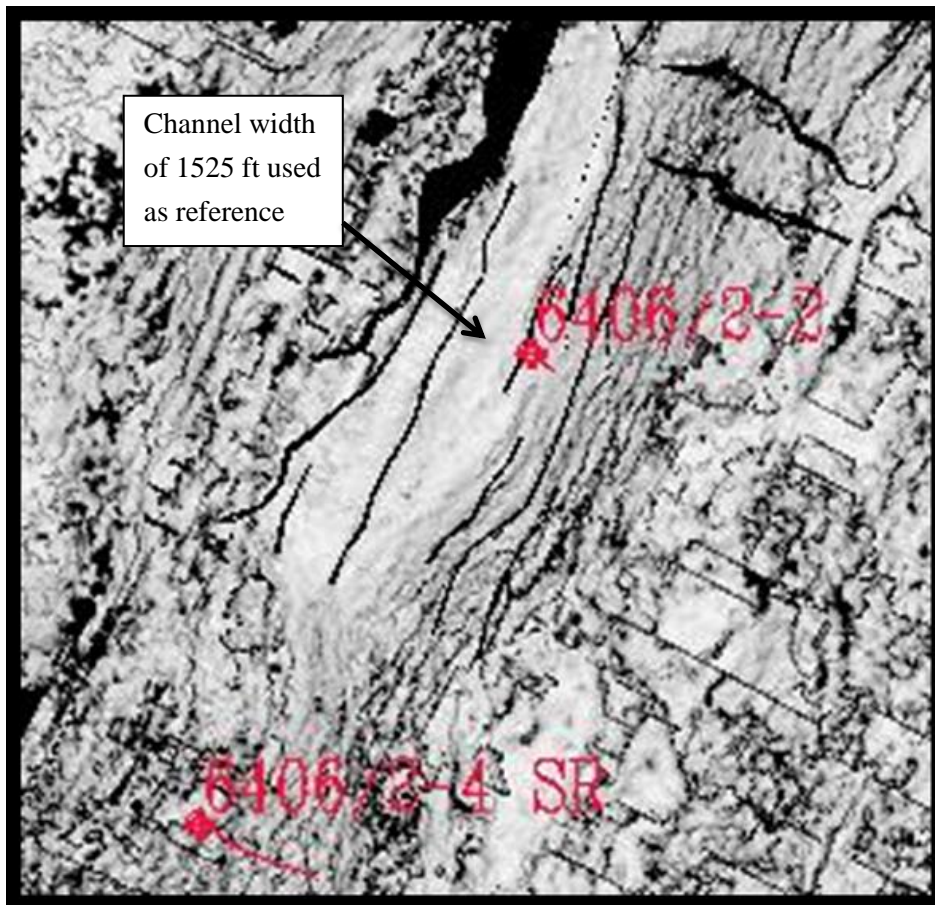


Figure 6: Location of 6406/2-2 and 6406/2-4SR in Lavrans

Well 6406/2-2

In well 6406/2-2 DST2 is used for re-interpretation together with geological information. DST2 perforation interval is located in Ile formation at 15462 ft – 15564 ft depth. DST 2 in well 6406/2-2 was run in March 1996. The well test consists of clean-up, short initial build-up, main flow and long final build-up. The test indicates two parallel impermeable boundaries, one on each side of the well. Permeabilities lower than arithmetic averages from core data. Bad borehole quality and/or semi-perforated formation may be present.

Good matches have previously been obtained, however in the absence of simple numerical modeling tool available today; models were quite extreme and inconsistent with geological data

A conventional PTA is done as a starting point before numerical models are interpreted.

Parameters used in models:

Permeability = 34 mD

Thickness = 36 ft

Flow capacity = 1230 mD·ft

Gas viscosity = 0.033 cp

Z factor = 1.0987

Gas volume factor = 0.00458 Rm³/Sm³

Total compressibility = 6.76E-5 1/psi

Porosity = 0.25

Reservoir pressure = 7439 psi (at gauge)

Reservoir temperature = 176 °C

Wellbore radius = 0.354 ft

Skin value = 0.60

Interpretation using conventional Pressure Transient Analysis

The log-log plot shows indication of parallel impermeable faults present near tested well. The analytical model is run with channel width set to 100 ft and 165 ft. As seen in *Figure 8* the match is ok when width of channel is 100 ft, but for both models the lack of flow restrictions (faults or compartments) are clear. This model is partially consistent with geological information. For further improvement a different model is needed, but then the consistency with geological map is lost.

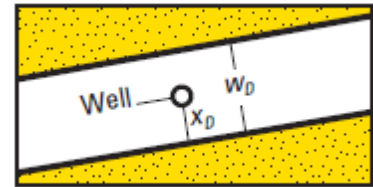
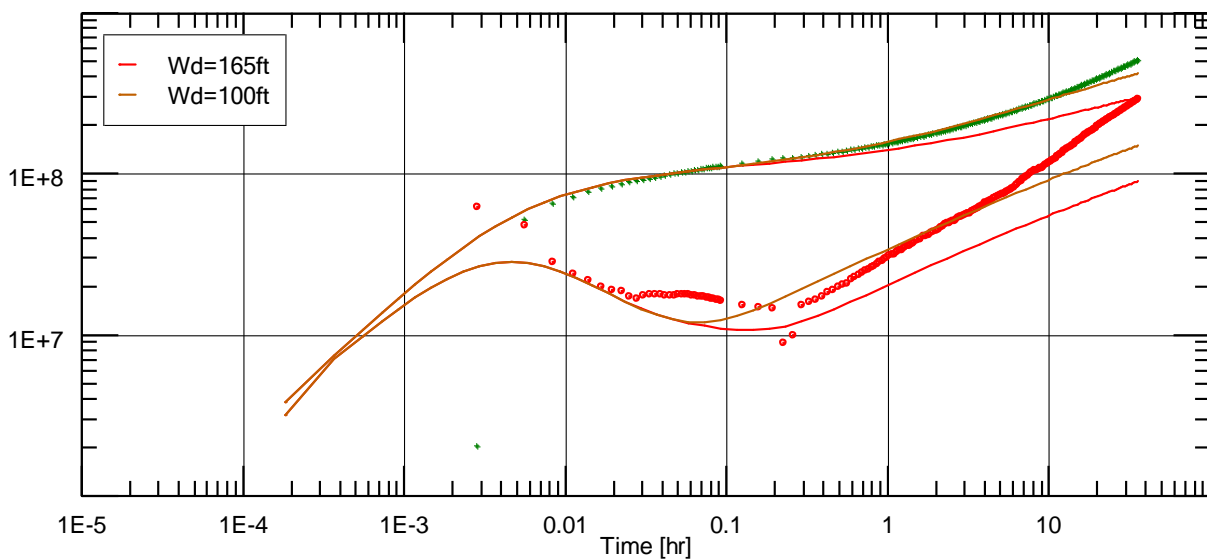


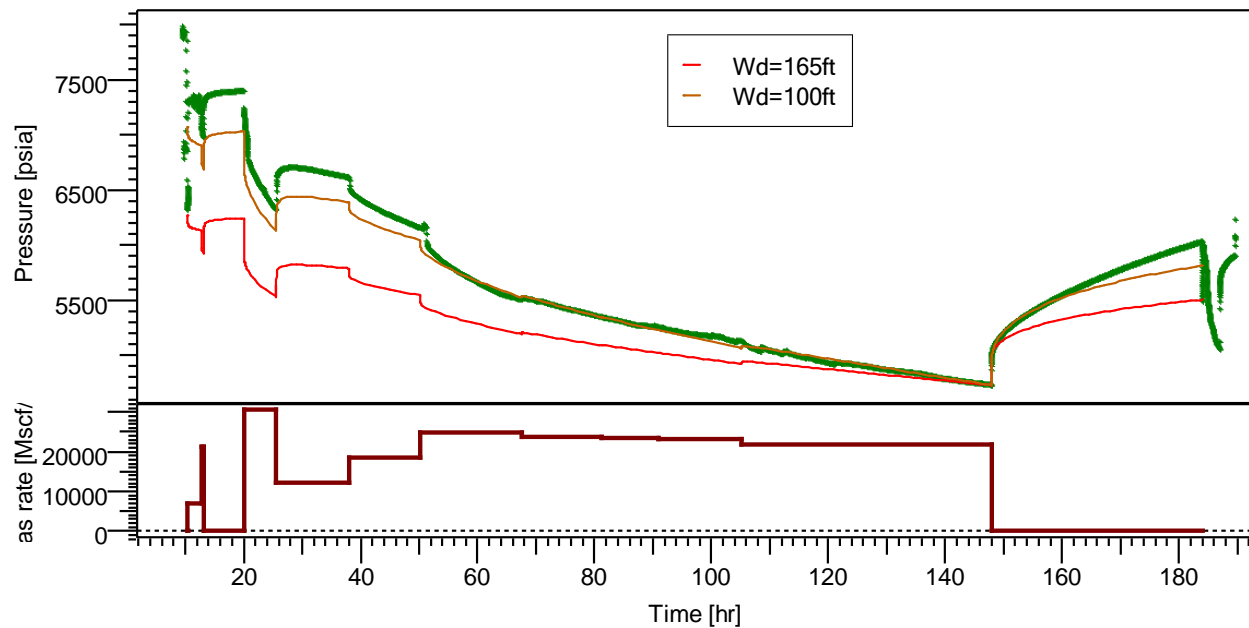
Figure 7: Well between two impermeable boundaries

Model show some WBS and skin effects, a trend of positive half slope and parallel faults. There are some wellbore/near-well effects present between 0.05 hr and 0.5 hr. Boundary effects are present.



Log-Log plot: $m(p) - m(p@dt=0)$ and derivative $[\psi^2/cp]$ vs dt [hr]

Figure 8: Log-log plot of well between two impermeable boundaries



History plot (Pressure [psia], Gas rate [Mscf/D] vs Time [hr])

Figure 9: History plot to Figure 8

Numerical

The geological map presented *Figure 6* is used as a reference for models and helps us decide which models that are realistic to use based on geological data available. Looking at PTT from DST2 the log-log plot is showing boundary effects, some skin effects and low wellbore storage. By using a geological map from Lavrans together with PTA software (Ecrin Saphire Kappa) and creating a new 2D map with existing faults a good match is obtained.

Following the clearly visible faults from geological map the match is not satisfying. Some boundary effects are clearly missing. Looking at the pressure response it is clear that the faults close to wellbore is the cause of pressure/rate falloff. Judging by the PTT response from faults drawn in after map it looks like permeability, skin and wellbore storage used in analytical model are consistent with values and results from this model. There may be one sealing fault close to the well on one side of the producing channel.

Composite model is used for some numerical analysis. A composite system is present if there is a change in mobility near well to a higher/lower value some distance from the well. The models are used with two different setups, one where permeability is constant and leakage through faults varies and a second where permeability varies from section to section. In the numerical model the leakage is treated as a transmissibility multiplier, with 0 implying fully sealing and 1 implying fully open (no restriction). Property changes are also handled through the use of multipliers. Looking at *Figure 10* the colors are regions (reg) with property changes and white the reference (ref) area. The composite regions are defined by:

$$M = \frac{\left(\frac{k}{\mu}\right)_{ref}}{\left(\frac{k}{\mu}\right)_{reg}}$$

$$D = \frac{\left(\frac{k}{\phi\mu c_t}\right)_{ref}}{\left(\frac{k}{\phi\mu c_t}\right)_{reg}}$$

And to keep porosity constant, the same values are used for M and D

$$\frac{(\phi c_t)_{ref}}{(\phi c_t)_{reg}} \rightarrow \frac{M}{D}$$

For the analytical approach a skin value of $S=-0.65$ was used for interpretation of well 6406/2-2. When numerical models are run there is a better match with, a higher, low positive value. A skin value of $S=0.6$ is found to give a good match on all models. Wellbore constant $C=0.013$ bbl/psi is found to give a good match. Porosity and thickness are kept constant in all models while permeability is for most models kept constant at 34 md. One composite model contains two or more zones where permeability change through the zones, i.e. section one has permeability p_1 and section 2 has permeability p_2 and so on. In the numerical model there are faults between each segment which will act as flow restrictors, but only over that point/line.

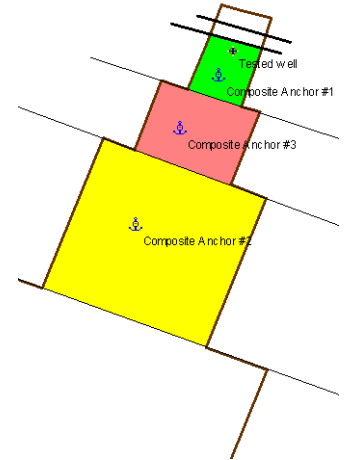


Figure 10: Composite model in well 6406/2-2

Composite model not consistent with geological map

For the numerical analysis several different models are generated and evaluated. From the analytical interpretation the same composite model is reconstructed using same parameters, lengths and widths. The closed reservoir is generated from model in *Figure 11*.

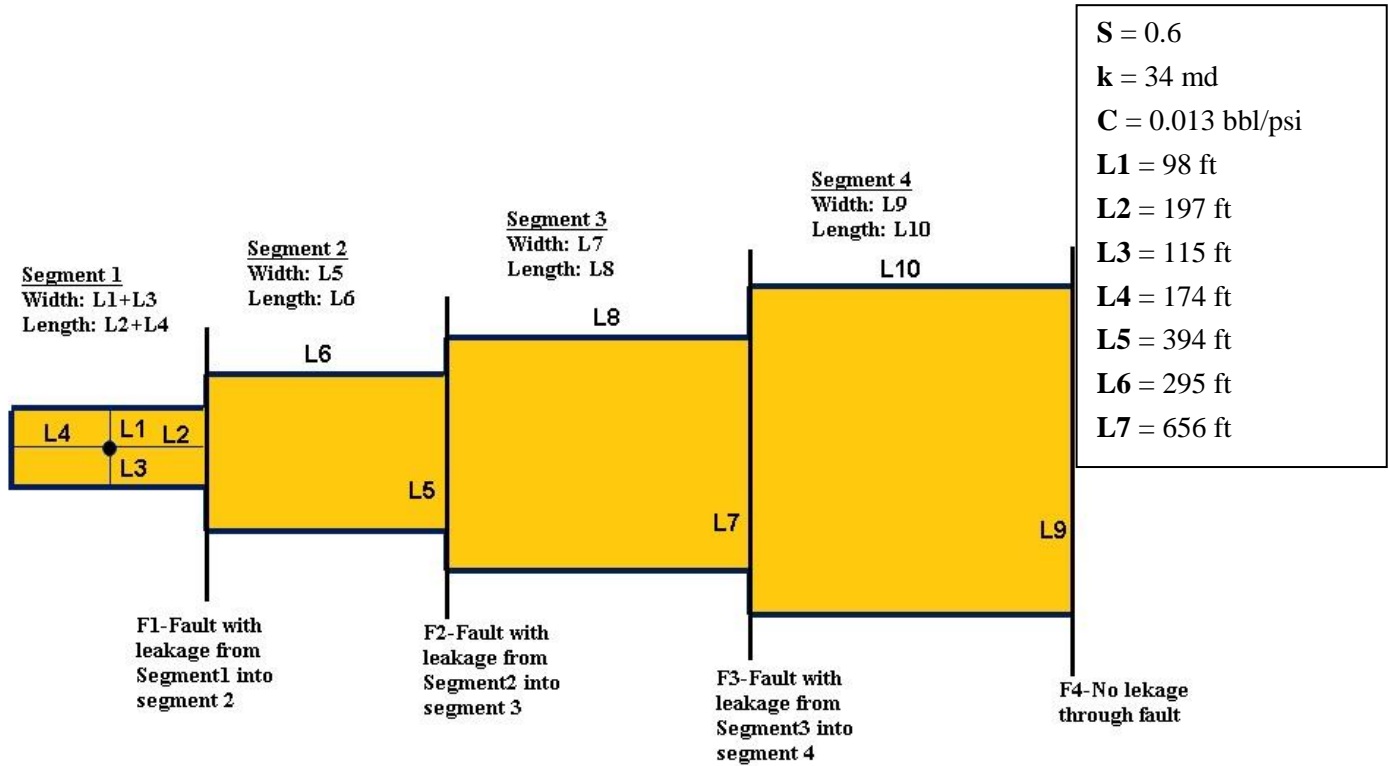
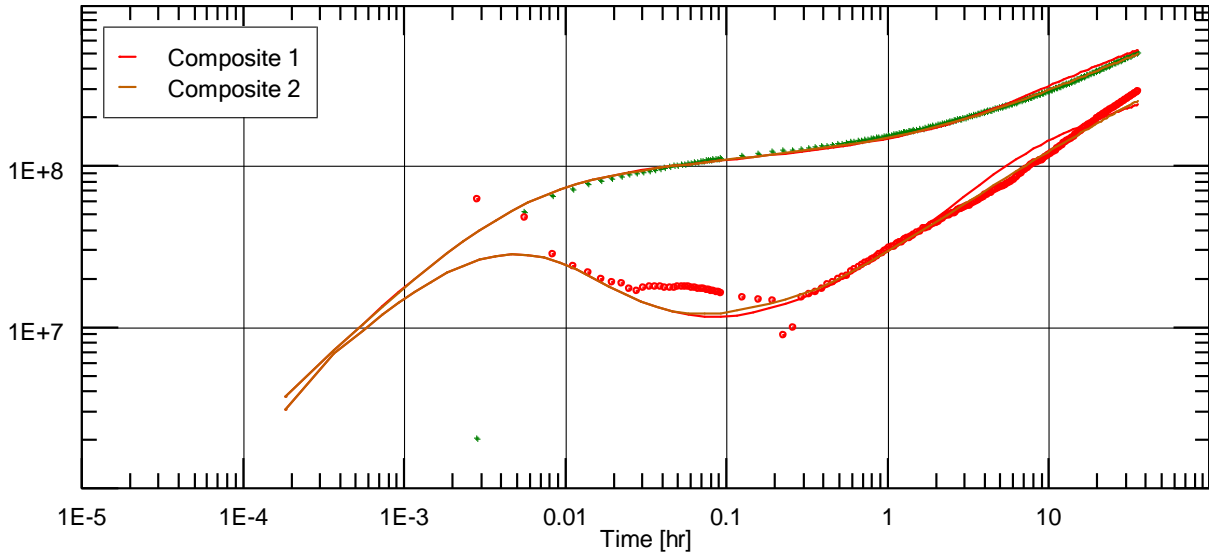


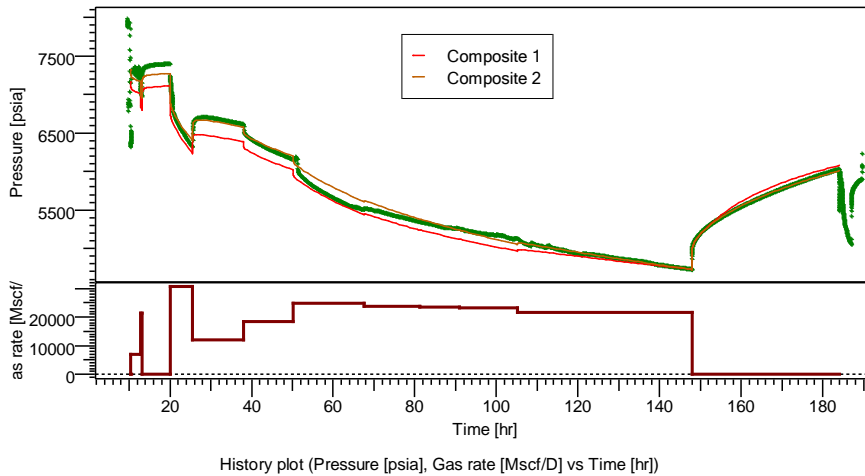
Figure 11: Segments width and length for Composite model used in well 6406/2-2

The first model is run with same parameters as in analytical model, with outer impermeable boundaries and permeable boundaries between segments. Some adjustment to the model is needed to obtain a good match. This model will give a wrong picture of the reservoir and parameters due to the mismatch with geological data; this is seen in *Figure 12*. Models like this may be chosen for analyzing this reservoir for several reasons. First, there may be restrictions in analytical software used for interpretation, so a composite model like the one in *Figure 11* is most consistent among available models. Another reason to use the model in *Figure 11* may be the lack of geological information, i.e. we have no previous insight into reservoir.



Log-Log plot: $m(p)-m(p@dt=0)$ and derivative $[\psi^2/cp]$ vs dt [hr]

Figure 12: Log-log plot of composite models.



History plot (Pressure [psia], Gas rate [Mscf/D] vs Time [hr])

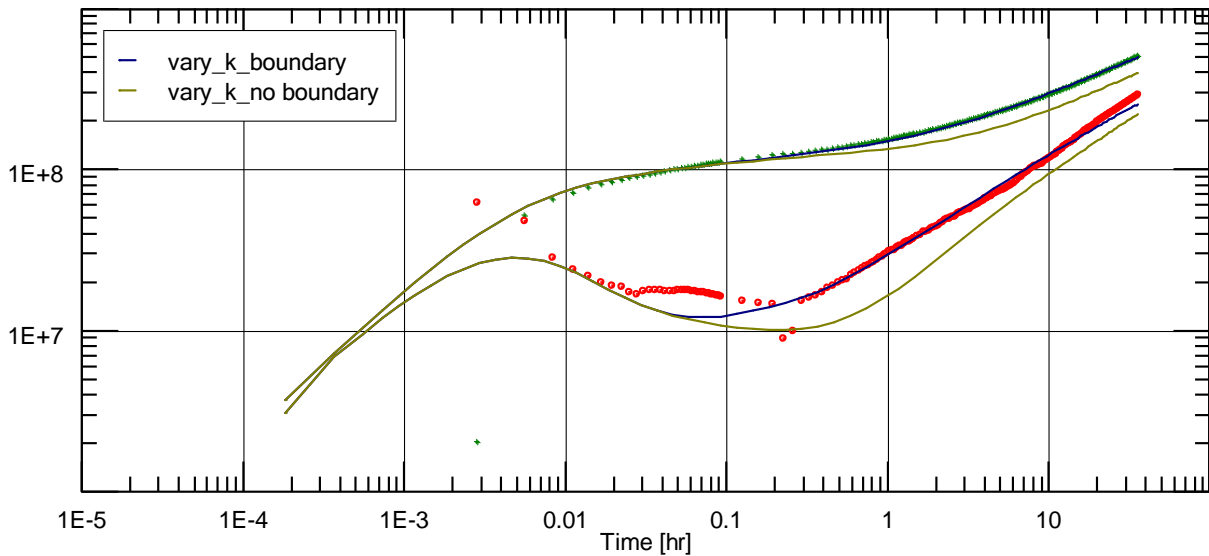
Figure 13: History plot to Figure 12

The composite model in Figure 11 is generated and run to show the great flexibility of numerical modelling. Sensitivity analysis is done on permeability within each segment (Composite 2) and on leakage through fault between the segments (Composite 1). To obtain a good match two different approaches may be used both with satisfying results. In the first model, *Composite 1*, permeability is set to be constant and leakage through faults separating segments is adjusted until a good match is achieved. Leakage through F1 and F2 must be set at low values to get a good match, 0.01 and 0.015 respectively. Further out the model opens up to early so effects further out are harder to identify which is also seen on

the model. In the second model, *Composite 2*, faults separating segments are 100% open and permeability within each segment adjusted until a satisfying match. $\frac{M}{D}$ for segments one, two and three are set to $\frac{1}{1}, \frac{3}{3}, \frac{7}{7}$ respectively, and the match is seen in *Figure 13*.

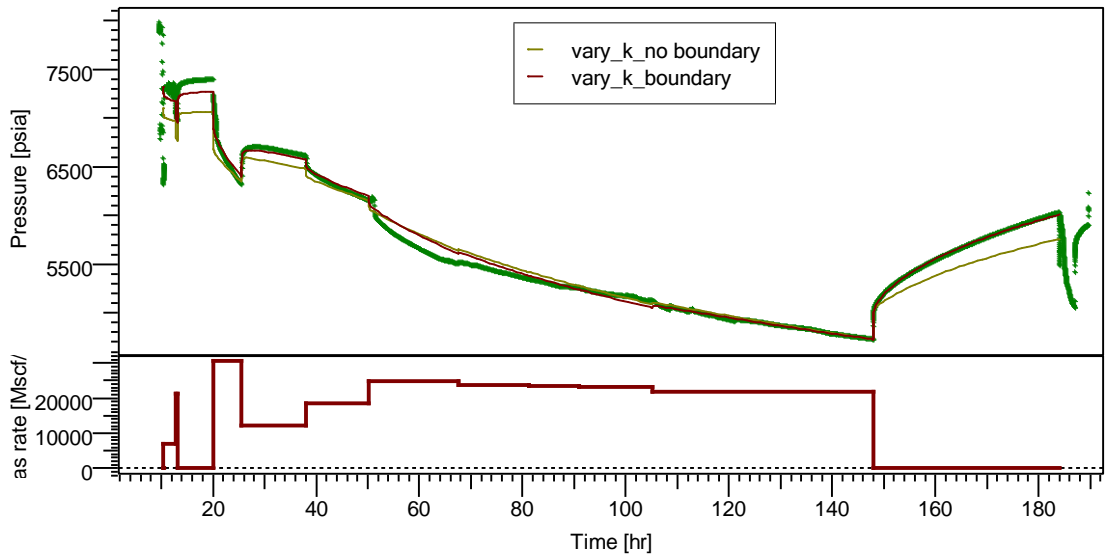
After running several models with sensitivity analysis it is safe to assume that near wellbore effects are present. By changing L4 from 174 ft to 50 – 80 ft there are clear improvements in pressure response. This effects and trends are shown in the log-log plot in *Figure 14*. The composite models with boundary show a much better pressure responds. Some faults between L4 and tested well may be present as matches improve, but any faults occurring in this area have a leakage of 0.1 or more. Sealing faults closer than 50 ft and further away than 80 ft (from well) show a negative trend in the pressure response.

When this composite model is laid on top of and compared to the geological map the early increase in width does not match the channel where tested well 6406/2-2 is located (*Figure 16*). Due to flexibility of numerical models we do still observe a good match on both log-log plot and history plot when composite model is run.



Log-Log plot: $m(p)-m(p@dt=0)$ and derivative $[\text{psi}^2/\text{cp}]$ vs dt [hr]

Figure 14: Log-log plot of composite model with varying k



History plot (Pressure [psia], Gas rate [Mscf/D] vs Time [hr])

Figure 15: History plot to Figure 14

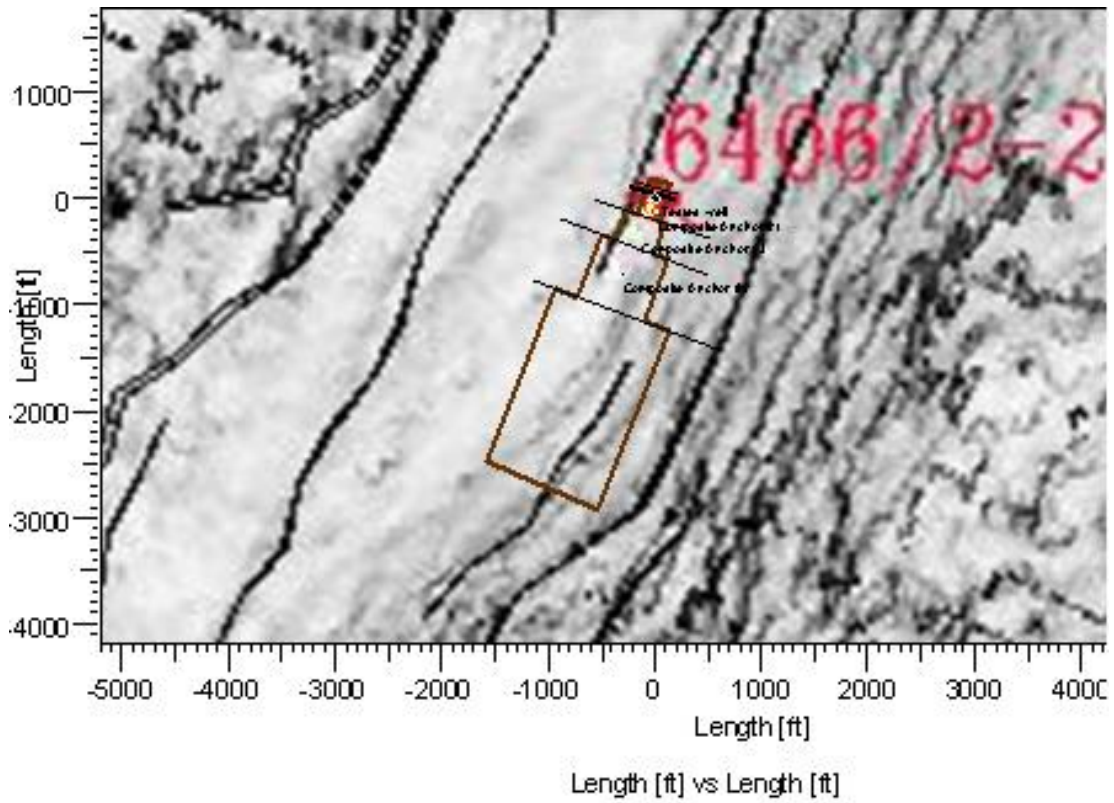


Figure 16: Composite model on geological map

Models based on geological map

First model: A new numerical model supported by geological data, with same width and length as channel on 2D map is created (*Figure 17*). The channel is 1050 ft long starting from the assumed sealing fault 80 ft north of the well, and the width of the channel is 160 ft. After 1050 ft of channel it looks like the formation is opening up, which are also consistent with other models. Adding and/or removing sealing faults at end of channel show the same indications. A positive skin value of $S=0.6$ and a permeability $k=34$ md is seen in *Figure 18* and give the best match and values are also consistent with other composite models run. The fault located 80 ft from well is impermeable, setting it to the smallest leakage a negative response show on both plots.

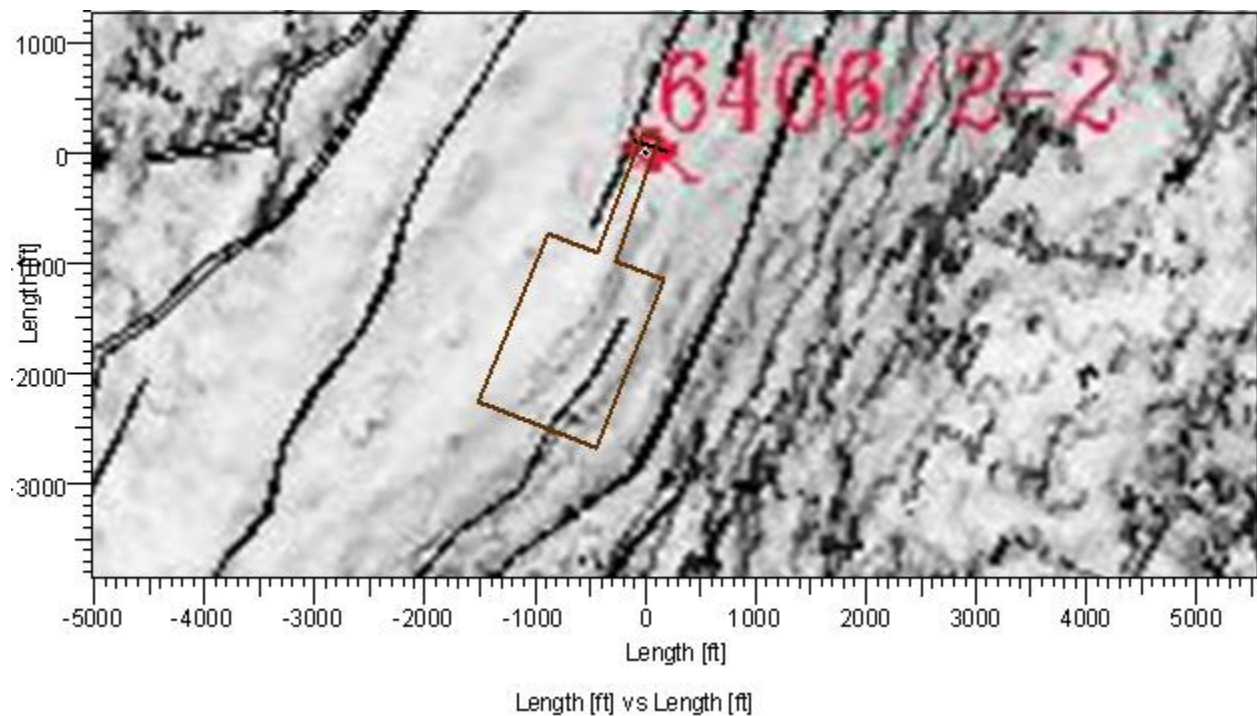
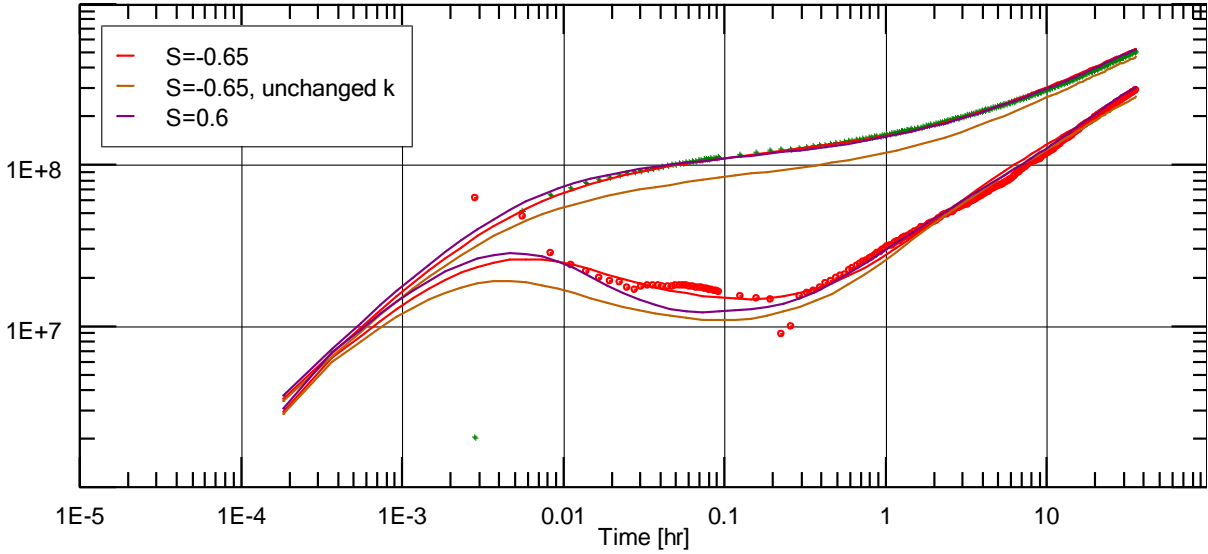


Figure 17: Truncated channel with well located north in the model, flowing from north to south

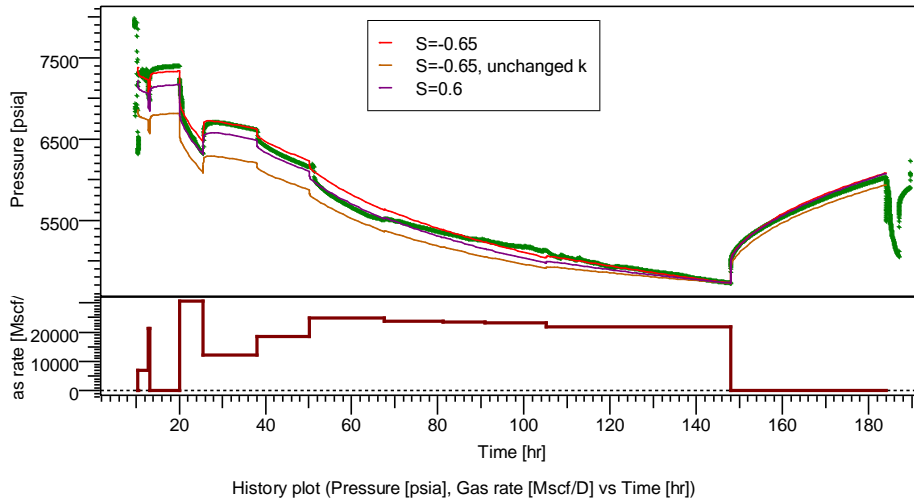
Taking a closer look at pressure response from $S=-0.65$ it is not as consistent as $S=0.6$, but with sensitivity analysis on permeability and set $k=28.4$ md the match is good. For $S=-0.65$ we must use a lower permeability of $k=24.8$ md and move near-well fault 30 ft further away which then give a ok match as seen in *Figure 18*. This is a good example on how flexible the numerical models are and how important it is to be critical when choosing models and values. If parameters for $S=-0.65$ and $S=0.6$ are set the same, $S=0.6$ give us a much better match. When laying models on top of geological map in *Figure 17* it is only partially consistent with geological information available. For better consistency with geological

information the model is closed on the one side and opened up equally on the other side. The pressure response stays unchanged and unaffected by the changes



Log-Log plot: $m(p)-m(p@dt=0)$ and derivative $[\text{psi}^2/\text{cp}]$ vs dt [hr]

Figure 18: Log-log plot of geological model in Figure 17, with three different skin values



History plot (Pressure [psia], Gas rate [Mscf/D] vs Time [hr])

Figure 19: History plot to Figure 18

Second model: In *Figure 20*, at end of channel, around 1050 ft, the formation is opening up in the west direction and following a fault on the east side for another 13 – 1600 ft. All faults surrounding channel are impermeable and making the channel a closed system until it opens up towards the end. There may be presence of some wider areas closer to the well, 30 ft – 50 ft wider the first 230 ft of the channel. Some flow restrictions towards the end of the channel before it opens up. In *Figure 21* the model from *Figure 20* is presented with impermeable boundary present 80 ft from wellbore (80 ft boundary), one 200 ft away from wellbore (200 ft boundary) and one without boundary (no boundary). The trend from log-log plot shows impermeable fault present close to the well.

It is not easy to identify any faults close to the well but all models show the same trend; decrease in channel width close to well running in the south-east direction. Following the channel north, we may have the same channel going 3-400m in that direction (sealing 50 – 80 ft south from well), but instead of opening up at end of channel the formation get more complex with faults present and after 500 m it's closing in giving a leakage of zero.

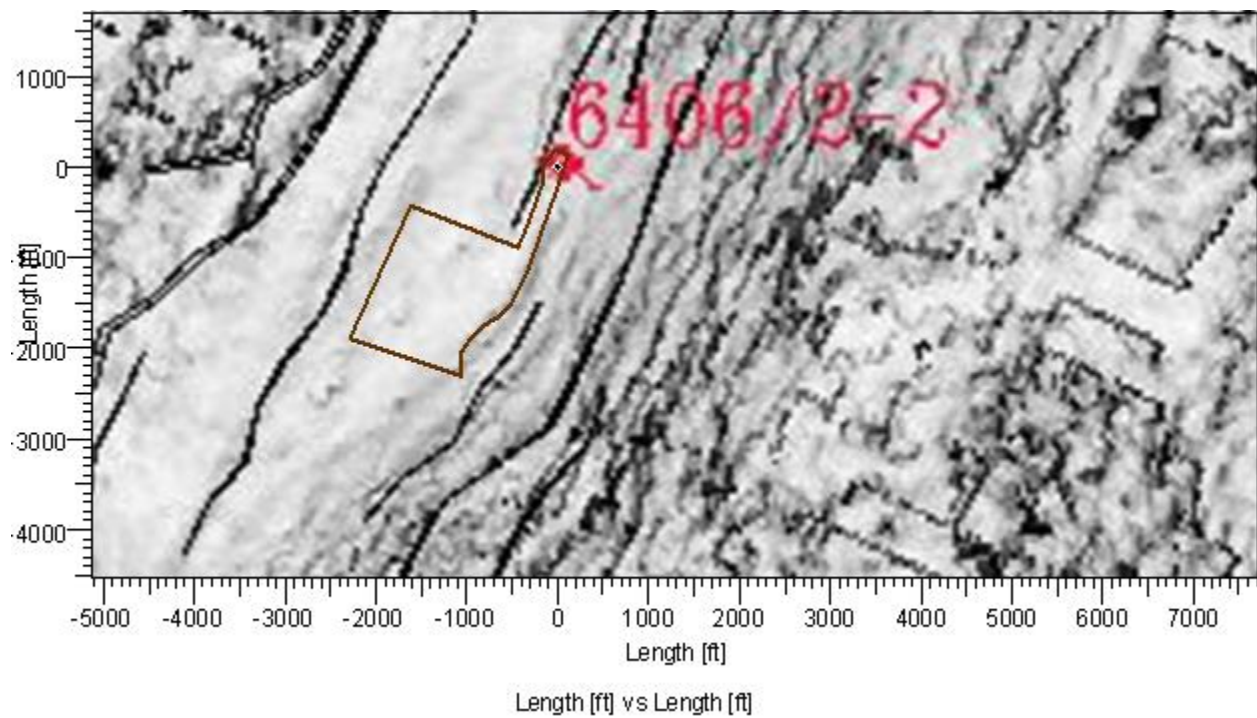
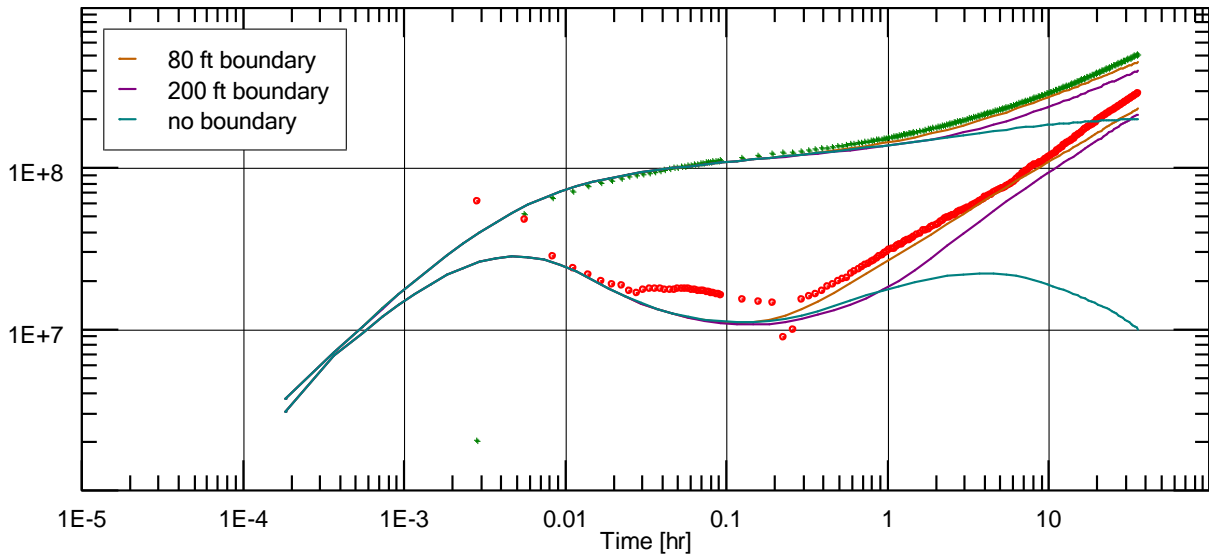
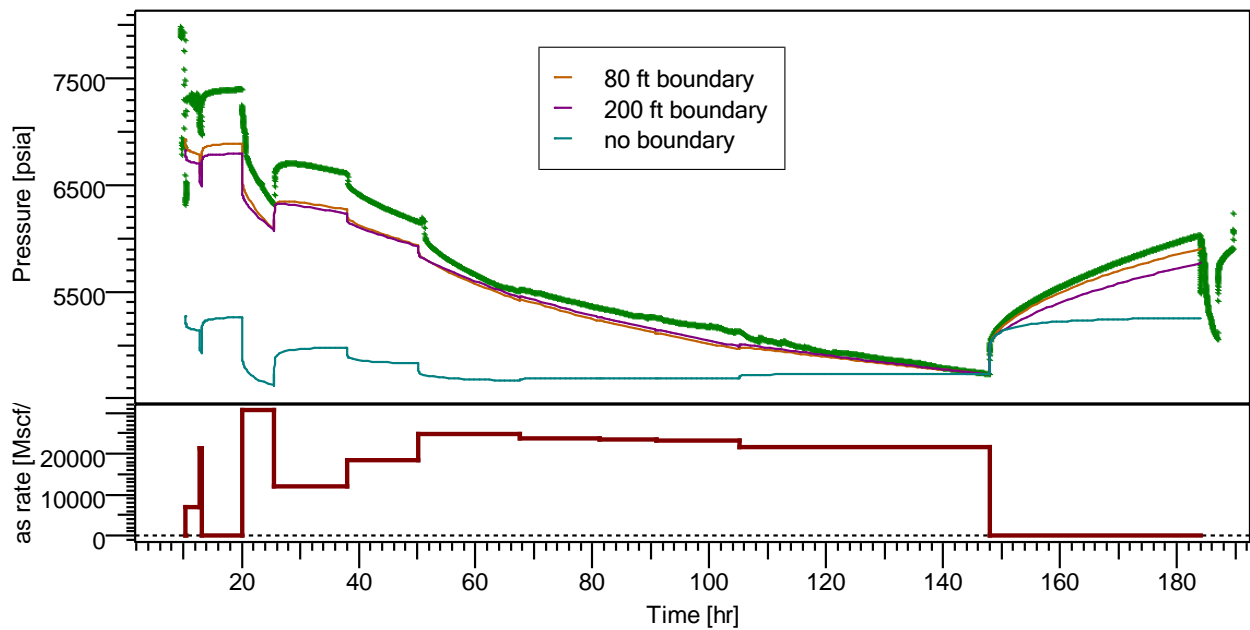


Figure 20: Truncated channel with well located north in the model, flowing from north to south



Log-Log plot: $m(p)-m(p@dt=0)$ and derivative $[\text{psi}^2/\text{cp}]$ vs dt [hr]

Figure 21: Log-log plot of geological model in Figure 20, fault effects



History plot (Pressure [psia], Gas rate [Mscf/D] vs Time [hr])

Figure 22: History plot to Figure 21

Third model: The model in *Figure 23* is one model assuming the channel, between two impermeable faults, is closed south from the location of well 6406/2-2. As seen on composite map the formation is more complex with several impermeable and permeable faults present. Pressure response is seen in *Figure 24* and is satisfying at early time but then deviates more as test continues. Model opens up earlier than expect from pressure response. For this model the indication of a truncated channel is good and pressure response improves when sealing off channel south from well.

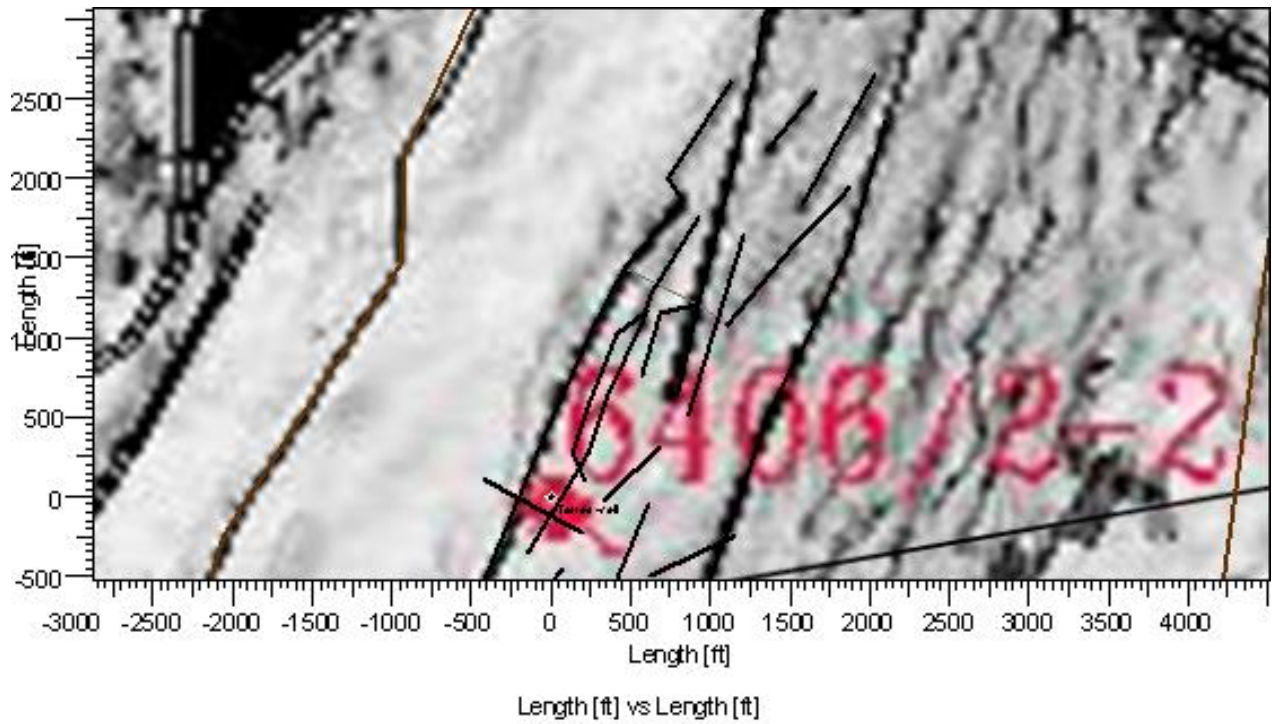
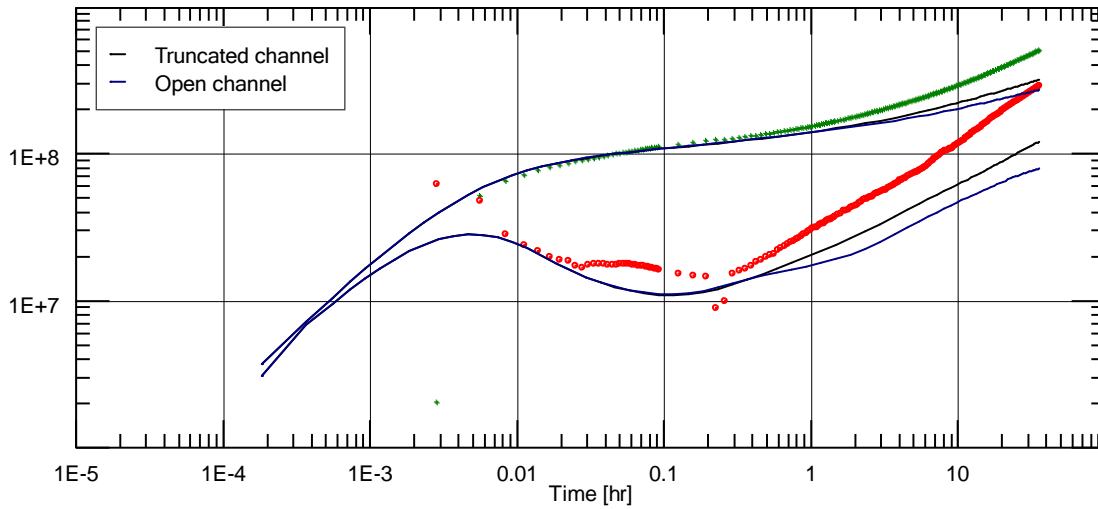
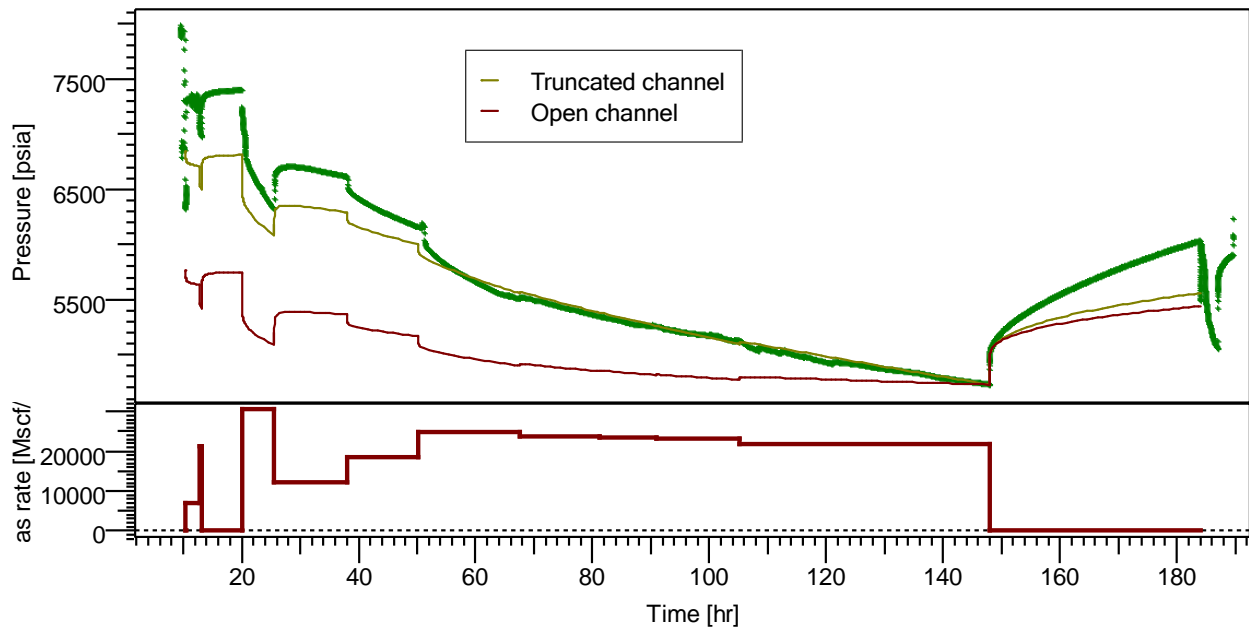


Figure 23: Model where channel is closed south from well and open in north direction



Log-Log plot: $m(p)-m(p@dt=0)$ and derivative $[\psi^2/cp]$ vs dt [hr]

Figure 24: Truncated channel vs open channel from model in Figure 23



History plot (Pressure [psia], Gas rate [Mscf/D] vs Time [hr])

Figure 25: History plot to Figure 24

Fourth model: The model in *Figure 26* is the model most consistent with geological map, assuming the channel, between two impermeable faults, is closed north from the location of well 6406/2-2. Geological map confirm that the formation is less complex and opening up after 1050 ft. There is also a good trend in pressure response after narrowing in channel close to the end (65 ft – 80 ft for 65 ft) just before. For this model the indication and trend of a truncated channel is good and pressure response improves when sealing off channel south from well. The response for truncated and open channel is seen in *Figure 27*.

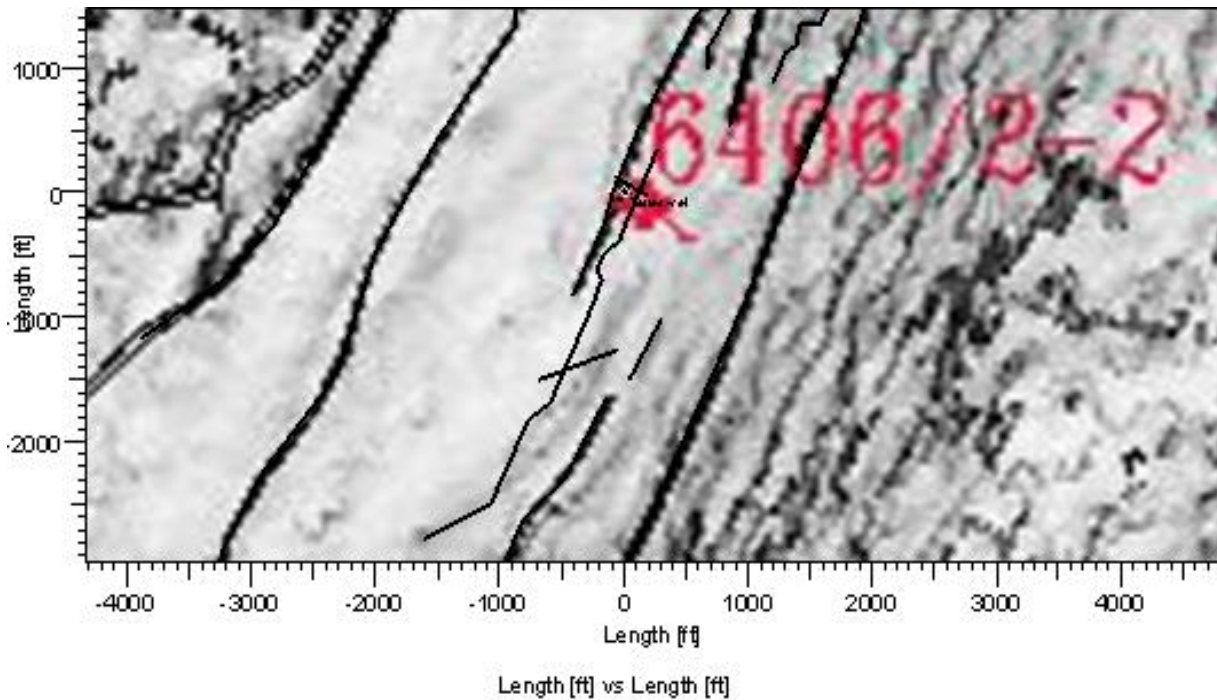
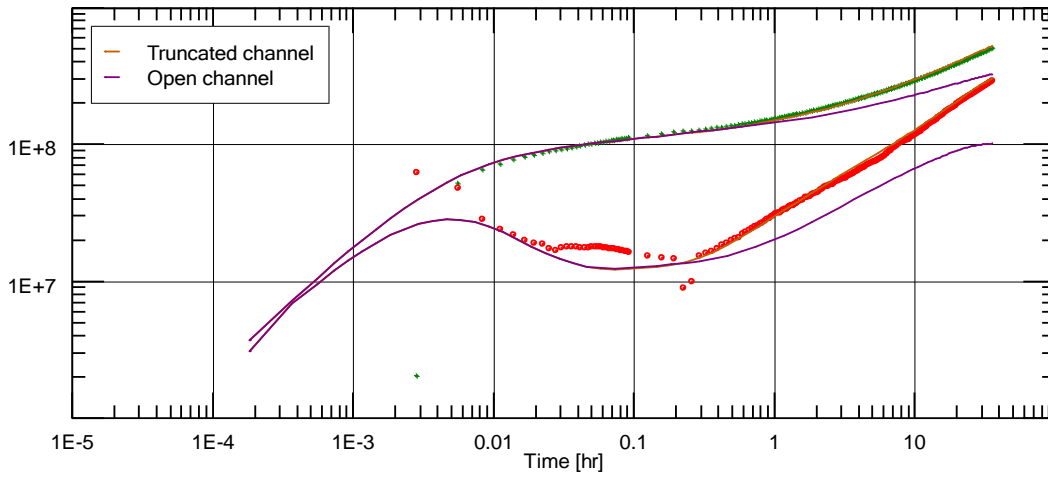
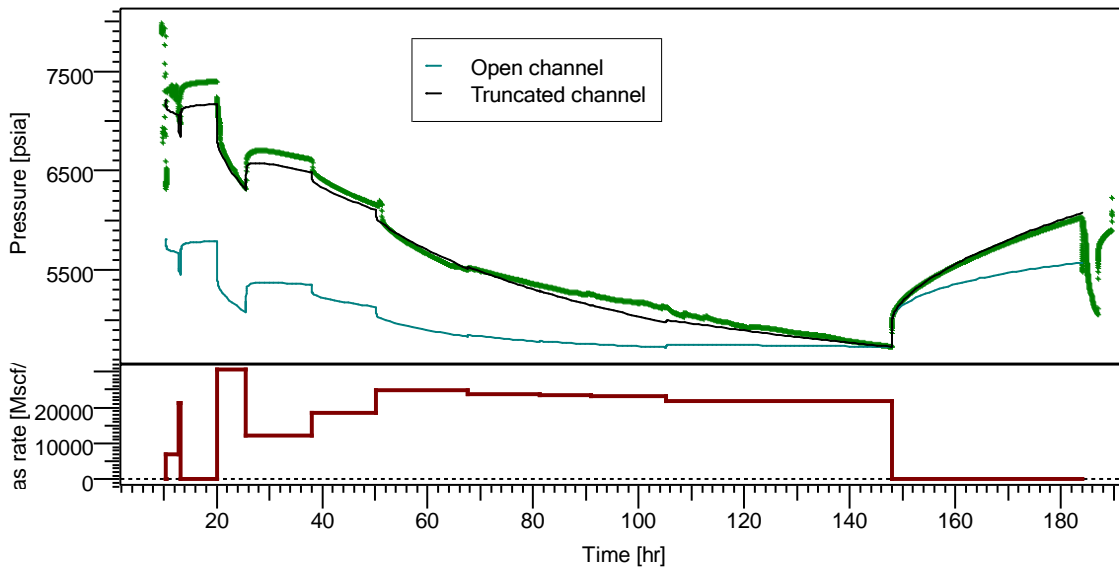


Figure 26: Model where channel is closed south from well and open in north direction



Log-Log plot: $m(p)-m(p@dt=0)$ and derivative $[\psi^2/cp]$ vs dt [hr]

Figure 27: Truncated channel vs open channel from model in Figure 26



History plot (Pressure [psia], Gas rate [Mscf/D] vs Time [hr])

Figure 28: History plot to Figure 27

Well 6406/2-4SR

In well 6406/2-4SR DST 1 is used for re-interpretation together with geological information. DST 1 perforation interval is located in Tilje formation at 15987 – 16085 ft depth. DST 1 in well 6406/2-4SR was run in January 1999. The well test consists of clean-up, initial build-up, main flow and final build-up. The test indicates complex boundaries around the well, with permeabilities lower than arithmetic averages from core data. Bad borehole quality and/or semi-perforated formation may be present.

Good matches have previously been obtained, however in the absence of simple numerical modeling tool available today; models were quite extreme and inconsistent with geological data

A conventional PTA is done as a starting point before numerical models are interpreted.

Parameters used in models:

Permeability = 14.5 mD
Thickness = 98.4 ft
Flow capacity = 1427 mD·ft
Gas viscosity = 0.037 cp
Z factor = 1.0987
Gas volume factor = 0.00458 Rm³/Sm³
Total compressibility = 6.89E-5 1/psi
Porosity = 0.156
Reservoir pressure = 7456 psi (at gauge)
Reservoir temperature = 168 °C
Wellbore radius = 0.354 ft
Skin value = 2.0

Interpretation using conventional Pressure Transient Analysis

The log-log plot from DST 1 shows indication of intersecting impermeable faults present near the tested well. The analytical model is run with the well centered $\theta_1 = 22.5^\circ$ (for $\theta = 45^\circ$), $r_D = 6.5 ft$ and θ set at 5, 45 and 90 degrees. As seen in *Figure 30* the match is not to good, but the trend show that impermeable boundaries are close to wellbore as the match improves at smaller θ . For this case the well lack some flow restrictions (faults or compartments) are clear and model is only partially consistent with geological information.

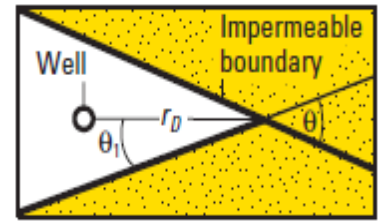
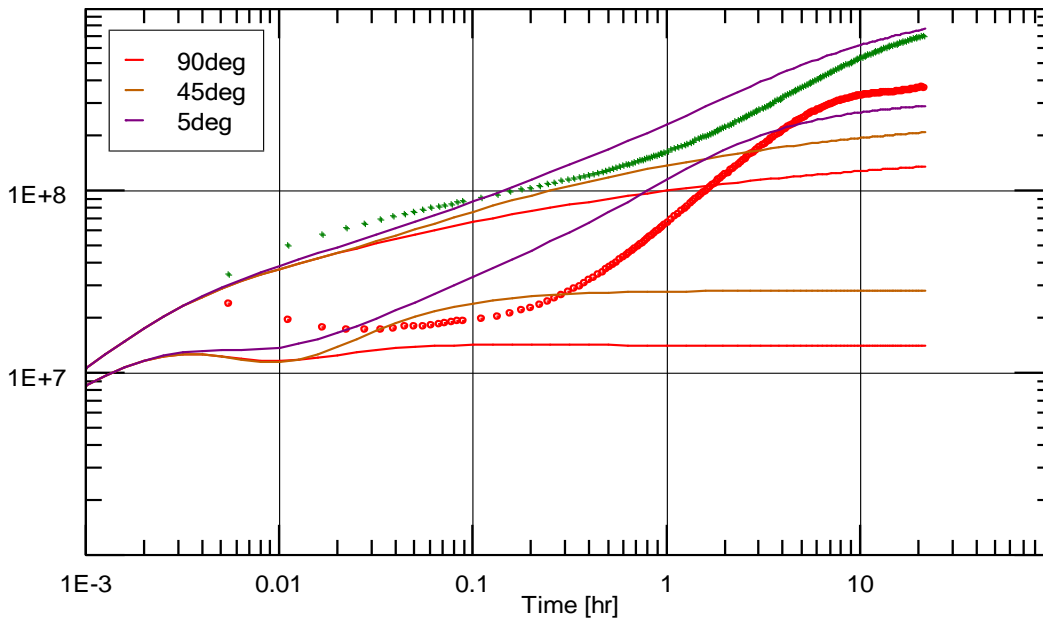


Figure 29: Well between two intersecting impermeable boundaries

Model show some WBS and skin effects, early time linear flow has a positive half-slope trend in derivative curve. Late-time linear flow.

For further improvement a different model is needed, but then the consistency with geological map is lost.



Log-Log plot: $m(p)-m(p@dt=0)$ and derivative $[\text{psi}^2/\text{cp}]$ vs dt [hr]

Figure 30: Log-log plot of well between two intersecting impermeable boundaries

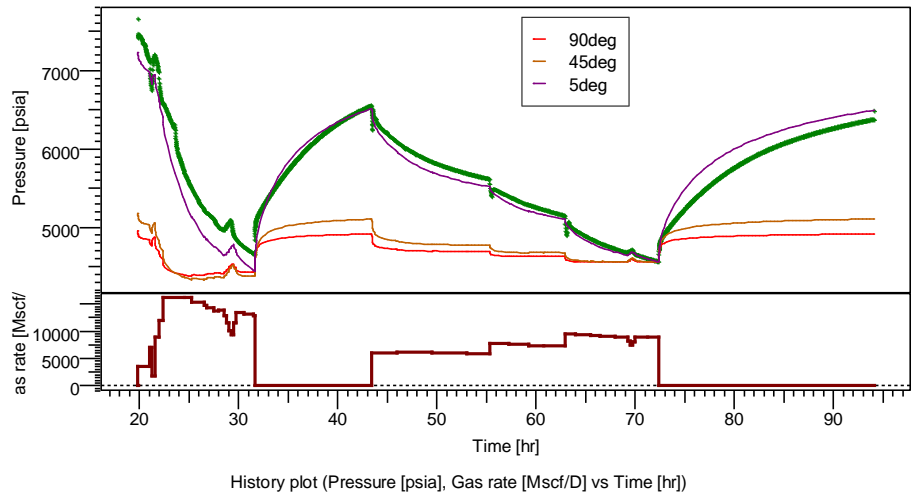


Figure 31: History plot to Figure 30

Numerical

The geological map presented in *Figure 6* is used as a reference for models and helps us decide which models that are realistic to use based on geological data available. Composite models and a complex flow pattern through labyrinth models are generated.

First model: In *Figure 32* the composite model is presented on top of geological map for well 6406/2-4SR. The formation is tight around the well but due to the small size of model and resolution in geological map further zooming will result in white/no background. The map indicates many faults and fractures in formation around wellbore so this trend is assumed to be present in smaller scale as well.

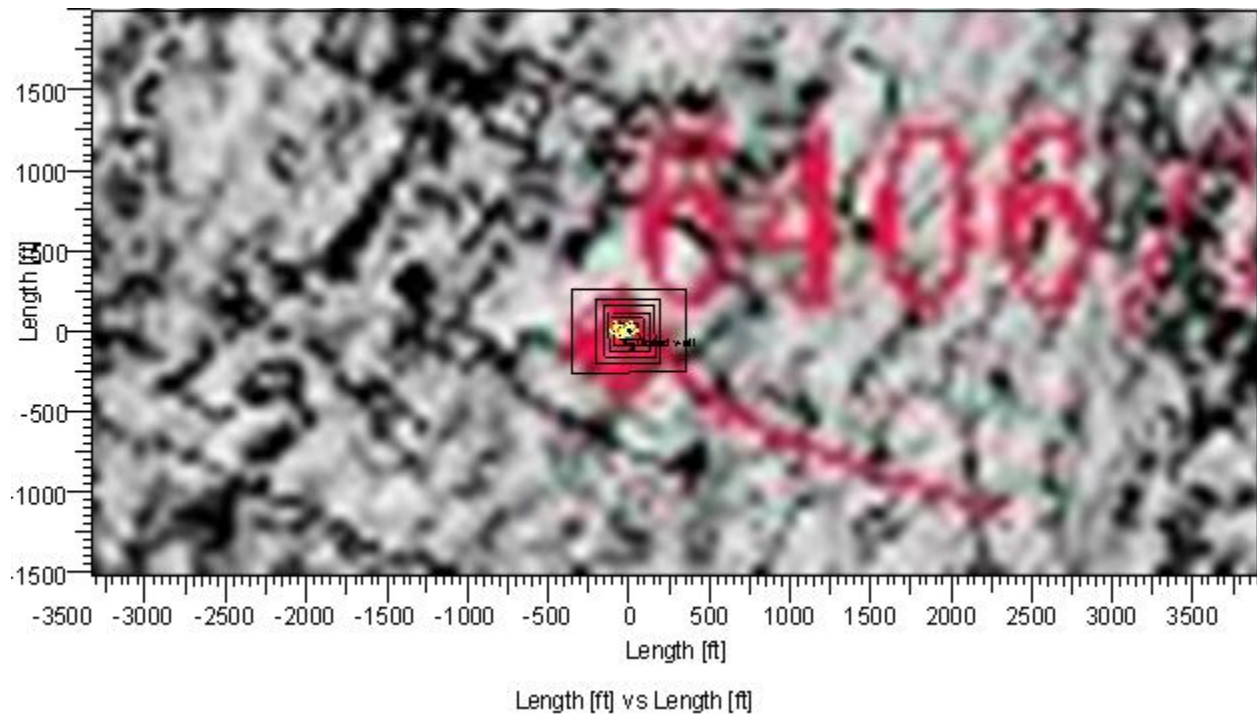
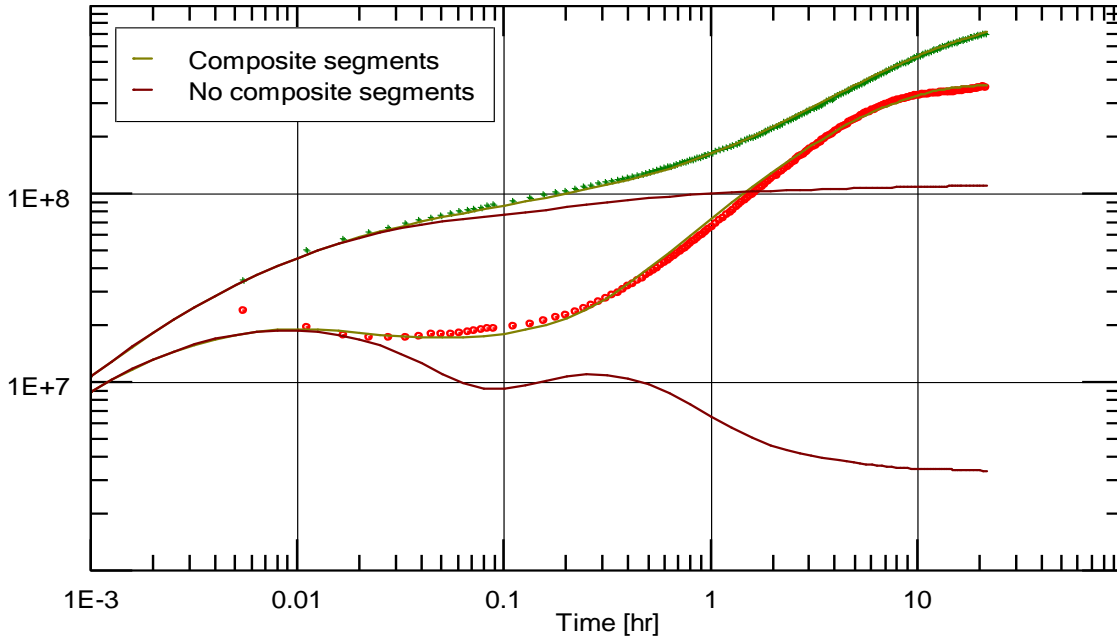


Figure 32: Composite model in well 6406/2-4SR

The composite model may as well be circular and giving us same results. The squared model was chosen to simplify construction and easier measure distances. Distances from the well and out to each of the four sides are roughly the same. Faults creating the side walls have been moved a short distance to check if results were affected, the results was unchanged. Log-log plot of composite model is seen in *Figure 33*. The trend with complex formation surrounding the well is consistent with the pressure response.



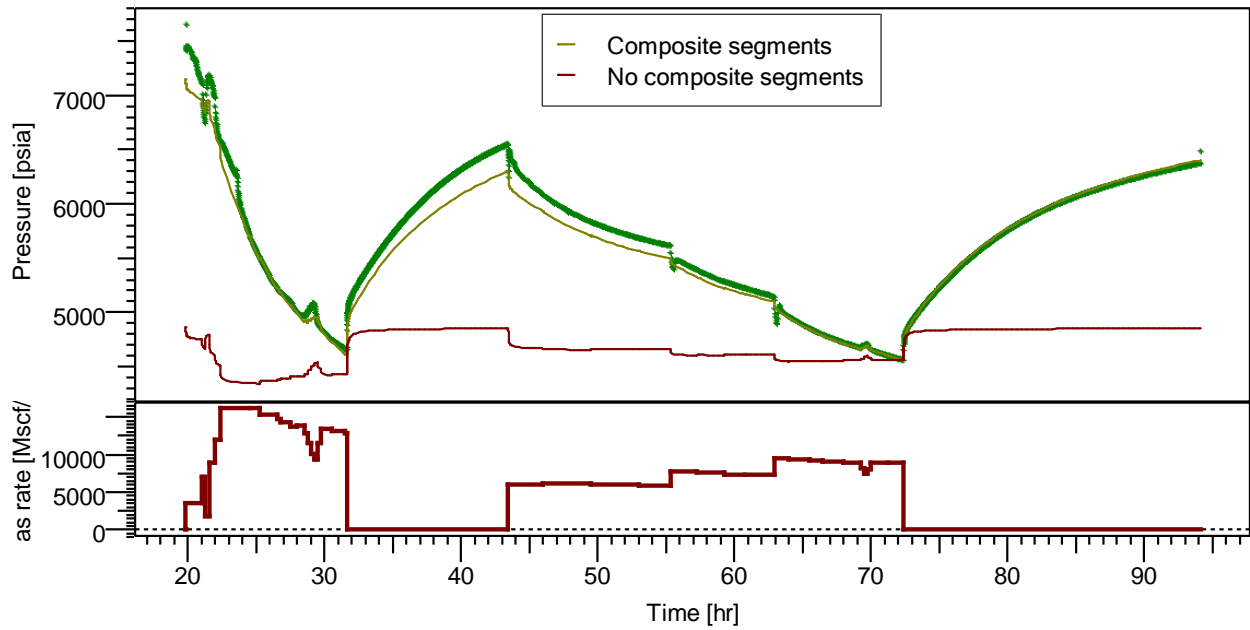
Log-Log plot: $m(p)-m(p@dt=0)$ and derivative $[\text{psi}^2/\text{cp}]$ vs dt [hr]

Figure 33: Log-log plot of composite model in 6406/2-4SR

Close to the wellbore there are several faults and compartments with lower permeability than reference permeability of 14.5 md. Skin is set to $S=2$ and WBS is set to $C = 0.0087$ bbl/psi. The first permeable fault is 6 ft from the well and the next three compartments (20 ft, 30 ft and 50 ft from well) also sealed by permeable (low leakage) faults. Within the first two compartments permeabilities are constant, only restricted by leakage over faults. The next four compartments have full leakage over faults separating compartments and decreasing permeability outwards within compartments. ($\frac{M}{D}$ for segments one, two, three and four are set to $(\frac{1.5}{1.5}, \frac{8}{8}, \frac{80}{80}, \frac{70}{70})$). After approximately 200 ft the model is opening up and no flow restrictions are present.

Due to the many compartments with reduced permeability and partially impermeable faults it is not much of the formation we see, which also may be expected from geological map.

An impermeable fault is added 50 ft from the well parallel to one of the sides. This fault gives an improved match on history plot so a sealing boundary close to the well may be present. On log-log plot there is no larger visible changes but the match here was already good and still is. The geological map indicates that there may be an impermeable boundary located south from the well.



History plot (Pressure [psia], Gas rate [Mscf/D] vs Time [hr])

Figure 34: History plot to Figure 33

Observing the two models plotted together, it is clear that without composite segments the match is way off. The model with segments present gives a good match and is consistent with geological data. All parameters for models are kept constant except from $\frac{M}{D}$ which is set equal to one for all segments in model without composite segments.

Second model: In *Figure 35* the position and a zoomed in version of the model showing flow pattern created in area around well. Several models with both more and less flow restriction are tried out, but model presented here give the best match. Parameters (k , S , C and *thickness*) are set to the same as in composite model.

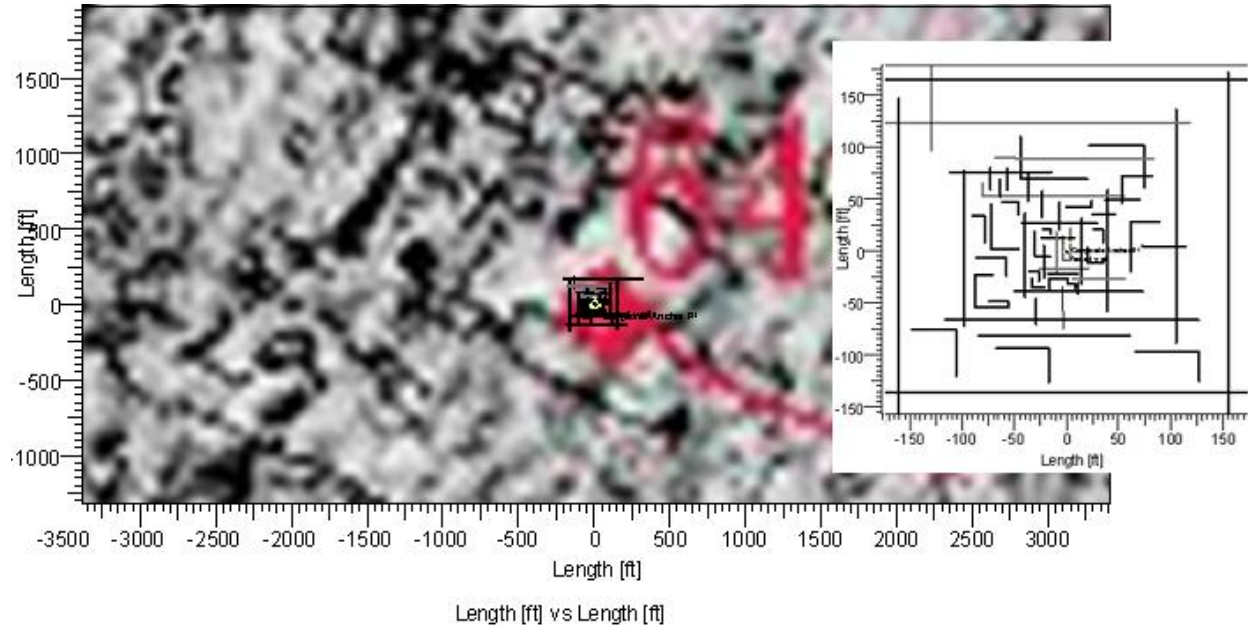


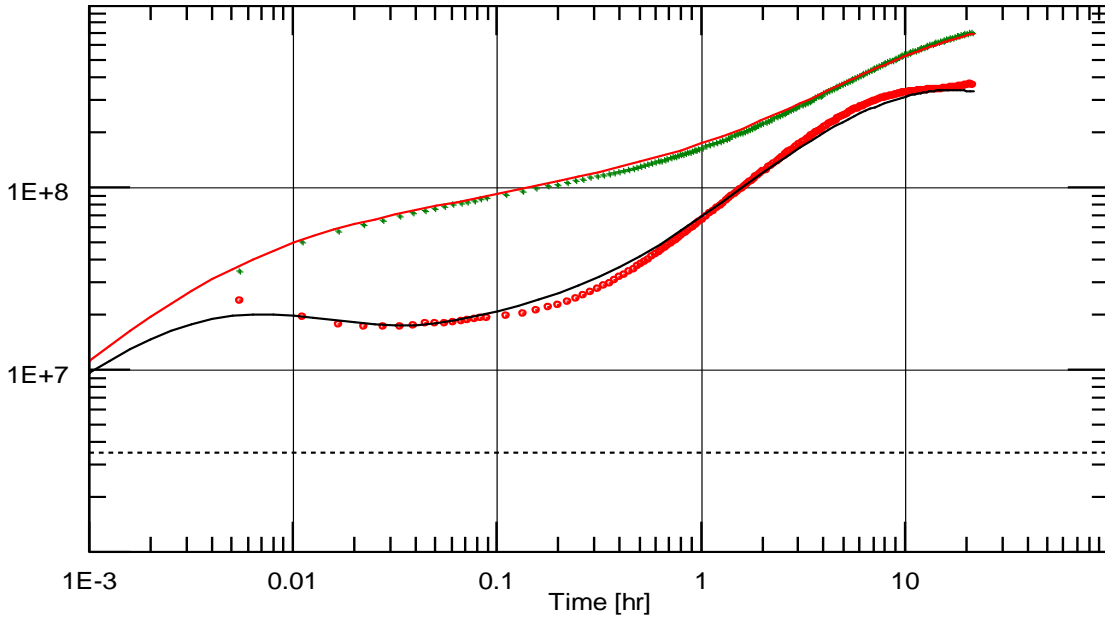
Figure 35: Labyrinth model in well 6406/2-4SR

The tested well is located in a composite area (10 ft * 15 ft) with $\frac{M}{D}$ for segment is set to $\frac{1.5}{1.5}$. The flow path continues in circles around itself with a channel width of 15 ft the first two straights before width doubles the next two straights. After that (around 60 ft in radius from location of the well) the model opens up both in channel width but also by leakage from the inner layers and outwards.

The model generated contains a high density of impermeable faults within the channels. Removing the impermeable faults within the channel is resulting in a clear mismatch.

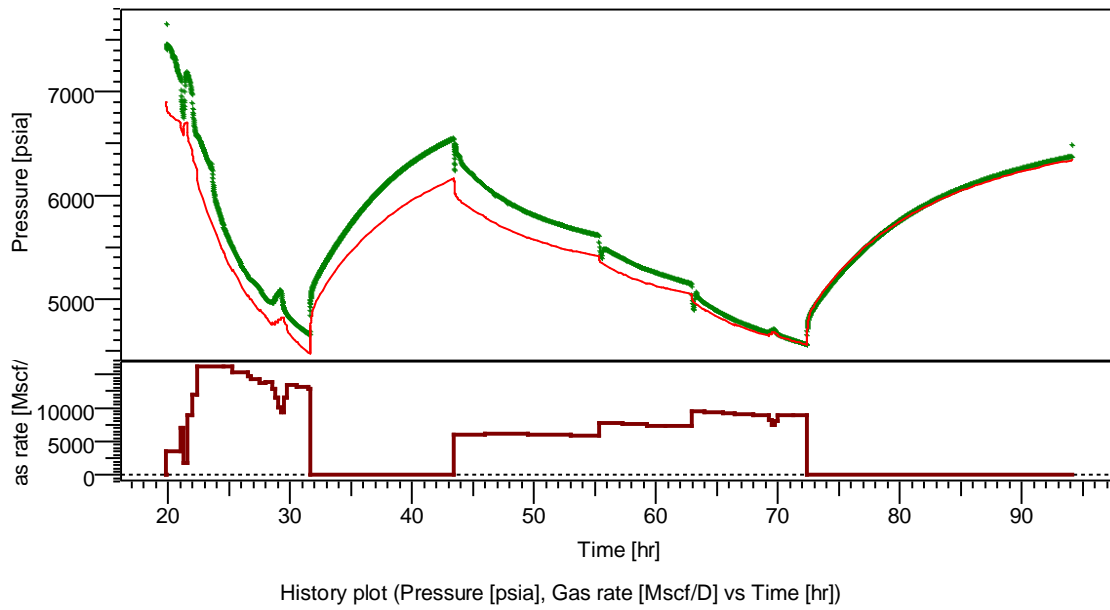
Several other models are tried out resulting in ok matches, but they all have the layout as model in *Figure 35* until radius reaches 50 ft from the well. After reaching 50 ft all models show the same trend being that channel tightens for some feet, opens up again before closing in and also containing some flow restrictions towards the end.

The match in *Figure 36* is good. The log-log plot show that there should be less flow restrictions between 0.1-0.4 hr and models may close in a bit more towards the end before opening up again.



Log-Log plot: $m(p)-m(p@dt=0)$ and derivative $[\text{psi}^2/\text{cp}]$ vs dt [hr]

Figure 36: Log-log plot of second labyrinth model in 6406/2-4SR



History plot (Pressure [psia], Gas rate [Mscf/D] vs Time [hr])

Figure 37: History plot to Figure 36

Third model: The model in *Figure 38* is located in the same part of the formation as the second model. The first 50 ft (radius) is unchanged from the second model, but instead of continuing around the well the flow is directed north through a channel surrounded by impermeable faults. Towards the end of channel some flow restrictions are present. The history plot show the same trend, that the model is opening up a bit too much towards the end.

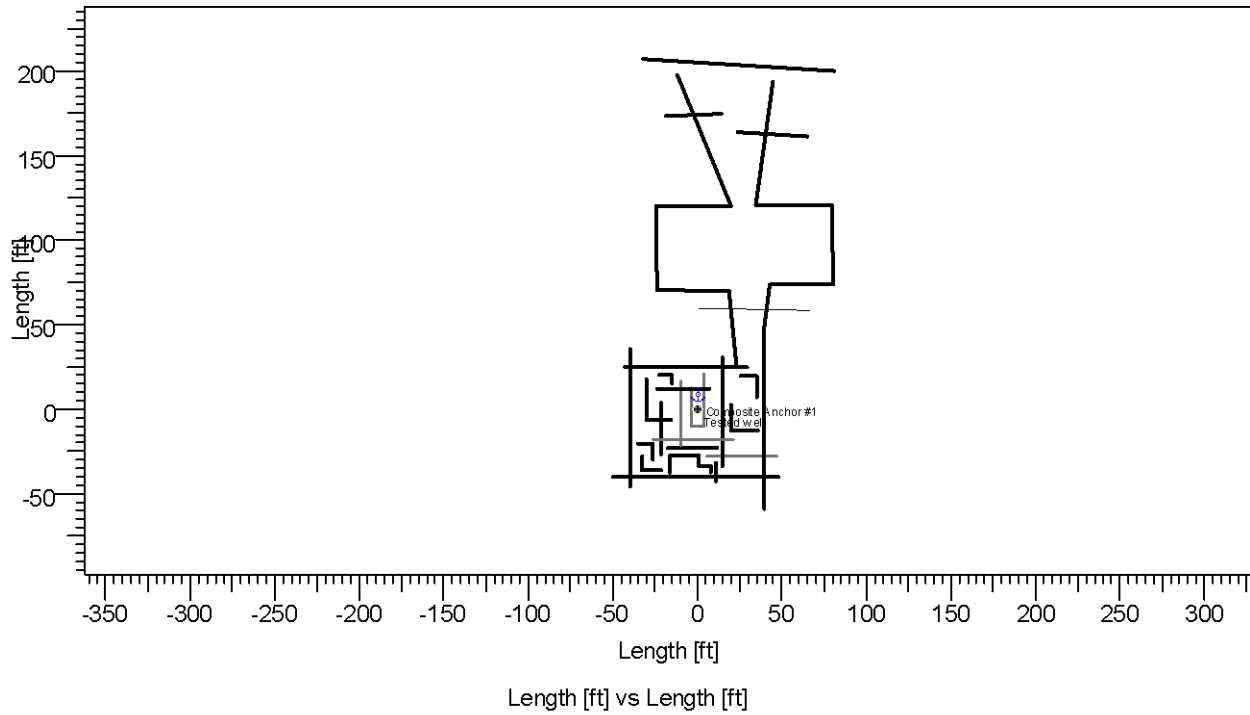
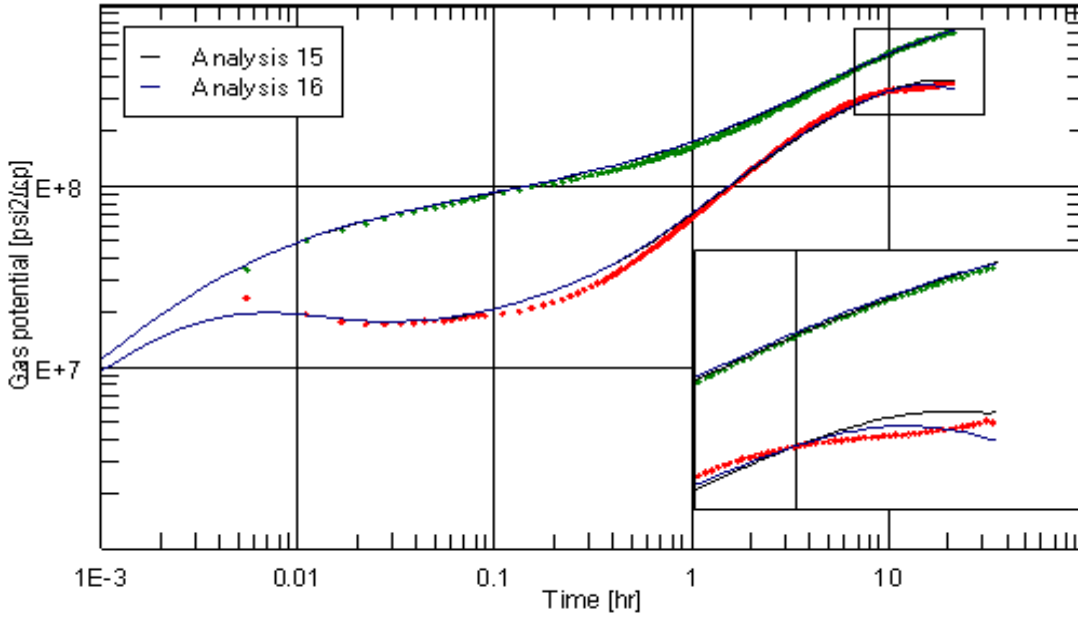


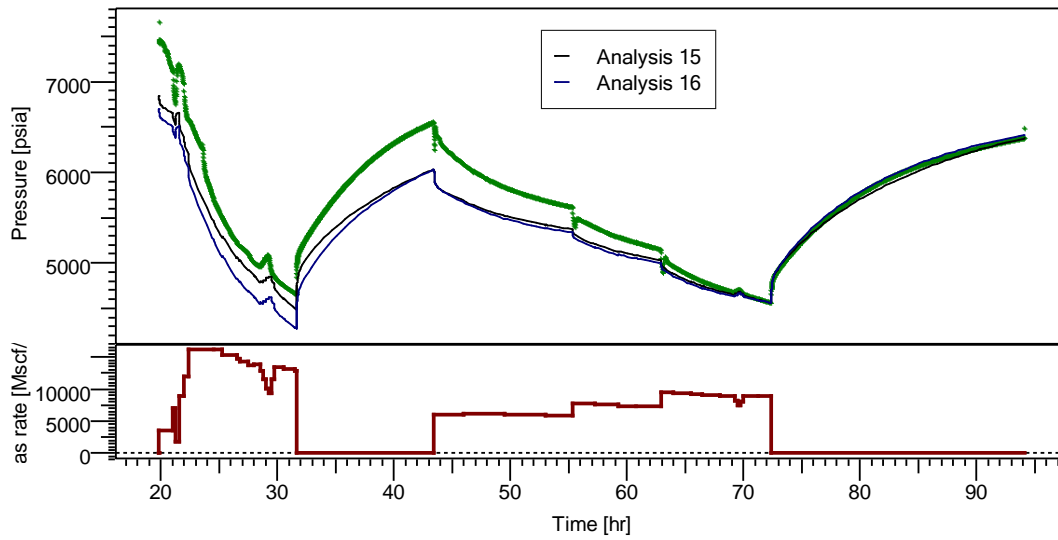
Figure 38: Third labyrinth model in 6406/2-4SR

From log-log plot in *Figure 39*, *Analysis 15* is the model with boundaries and *Analysis 16* is the model without boundaries towards the channels end. The same trend is observed here, lack of flow restriction at the end of the model.



Log-Log plot: $m(p) - m(p@dt=0)$ and derivative [psi²/cp] vs dt [hr]

Figure 39: Log-log plot of third labyrinth model in 6406/2-4SR



History plot (Pressure [psia], Gas rate [Mscf/D] vs Time [hr])

Figure 40: History plot to Figure 39

5 Conclusion and recommendation

Numerical models have been generated for two DST's run in the Ile and Tilje formations in the exploration wells 6406/2-2 and 6406/2-4SR in the Lavrans field. One of the main goals with this thesis was to identify new possible flow patterns existing in formation around the different wells. Several models, with basis in geological maps, are made for each formation and compared to geological data to confirm consistency.

5.1 Conclusion

Lavrans has many isolated segments and/or complex fault distribution throughout the formation; especially around well 6406/2-4SR in the Tilje formation. Numerical models give a good indication of possible flow patterns which is consistent with pressure response and geological data. Due to low resolution on geological maps it has not been possible to compare the more detailed models to geological data, but the wide complexity of formation is seen and observed in smaller scale through the numerical models.

6406/2-2

According to pressure trends all models show that well 6406/2-2 in the Ile formation (DST 2) is located in a truncated channel which is also consistent with geological data. The channel is easily located in map but it is not as wide as the map indicates, only 160 ft wide, and 50 ft – 80 ft north from the well an impermeable fault is present, sealing the channel in that end while it's open in the south going direction. After 1050 ft the channel opens up towards west. A composite model for 6406/2-2 DST 2 was run to show the flexibility of the numerical models and also underline how important it is to be critical when choosing models.

6406/2-4SR

Series of numerical models were run for DST 1 in well 6406/2-4SR in the Tilje formation to recognize and understand formation near and around wellbore. It is found to be a complex formation with several permeable and impermeable faults and compartments surrounding the well. Two possible models are found to give a good match. One composite model with compartments of different permeability built outside the previous compartment. The second model is a flow channel going in circles around the well varying in width of the channel, also with several permeable and impermeable faults present in channel. It is hard to say that one model is more likely to be present than others without more geological information (e.g. higher resolution on geological map).

Second and third model give satisfying matches and even though the second model is a bit creative they are both realistic. The third model is simpler and may be present with some variations. The models used

have one shape to show an example of one possible layout, but they may vary in shape and geometry and still provide satisfying matches. This is also shown by the second and third model. They are similar with a small radius from the well and differs as they expands (grow in size) further out.

5.2 Recommendation

For future work it would be interesting to gather more geological information to confirm the models generated. It could be log data, geological structure or sedimentology.

Deconvolution on existing data to see if it is possible to get a better match.

Production test may be something to consider which will also increase quality PTA.

References

Dolberg D.M., 2011, Porosity prediction from seismic inversion, Lavrans Field- Halten Terrace-Norway

Ecrin, Ecrin Kappa Sapphire version 4.30.05, Manual, Help topics and Tutorials

Gladfelter, R.E; Tracy, G.W. and Wilsey, L.E., 1955, "Selecting Wells Which Will Respond to Production-Stimulation Treatment," *Drill. And Prod. Prac.*, API, Dallas (1955) 117–29.

Gringarten, A.C., 1979, A Comparison Between Different Skin and Wellbore Storage Type-Curves for Early-Time Transient Analysis, SPE-8205-MS

Hawkins M., 1956, A note on the skin factor, Petroleum Transactions, AIME, vol 207, p356-357

Horne, R.N., 1995, Modern Well Test Analysis, 2nd ed. Palo Alto

Jun Y., Minglu W.: “Streamline numerical well test interpretation”, 2011

Kazemi H., Al-Ajmi N.M., Ozkan E.: “Estimation of Storativity Ratio in a Layered Reservoir With Crossflow”, (2008), SPE-84294

Kuchuk F., Biryukov D., 2014, Pressure transient behavior of continuously and discretely fractured reservoirs, *SPE-158096*

Kuchuk F.; Biryukov D., 2013, Pressure transient tests and flow regimes in fractured reservoirs, SPE-166296

Larsen L., 2010, Course compendium in Well Testing, University of Stavanger

Lehne, K.A., 2013, Course handout in Formation Evaluation, University of Stavanger

Norwegian Petroleum Directorate (NPD), Cited spring 2014, Information about wells, Available from: <http://factpages.npd.no/factpages/Default.aspx?culture=en>

Schlumberger, 2006, Fundamentals of Formation Testing, p163-185

Schlumberger, 2002, Well Test Interpretation, SMP-7086-5

Theis C.V., 1935, The Relation Between the Lowering of the Piezometric Surface and the Rate and Duration of Discharge of a Well Using Ground Water Storage, p519-524

Warren, J.E.; Root P.J., 1963, The Behavior of Naturally Fractured Reservoirs, SPEJ 426

Watson, A.T.; Gatens III, J.M.; Lane, H.M.: “Model selection for well test and production data analysis”, (1988), SPE-15926

Wei L. 2000. Well test pressure derivatives and the nature of fracture networks, *SPE-59014*

Larsen, L., spring 2014, The Lavrans Field, (Personal communication)

Shumakov, Y., spring 2014, Well test analysis, (Personal communication)